Introduction

Prognosis of pediatric acute lymphoblastic leukemia (ALL) has dramatically improved and recent clinical studies report excellent results for children [1–7]; however, the probability of survival of older children is unsatisfactory [7, 8]. The biological and molecular genetic features differ between older and younger children with ALL [9–14], such as higher frequency of poor prognostic factors, T-cell phenotype [12], *BCR-ABL1* translocations [14] and a lower frequency of favorable prognostic factors, including high hyperdiploidy and the *ETV6-RUNX1* translocation [13].

Thus, specific attention should be paid for older children with ALL, and pediatric-specific intensive chemotherapy could improve the outcomes of this group [8, 10, 15–19]. Although 15 years or older adolescents have been reported as a risk factor for poor outcome because of higher induction failure, relapse and therapy-related mortality [8, 15, 18, 20], there is limited information available regarding the characteristics of 15 years or older patients with ALL who underwent treatment in clinical studies [8, 11, 19]. Therefore, the optimal treatment for this age group is not established [21]. This situation occurs partly because such patients are treated by adult and pediatric oncologists, even though ALL is relatively uncommon in adolescents and young adults.

In the present study, we retrospectively analyzed the long-term outcomes of with ALL aged 10 years or older (younger-adolescents) who were enrolled in the three consecutive Tokyo Children's Cancer Study Group (TCCSG) ALL treatment protocols between 1995 and 2006. We focused particularly on children aged 15–18 years (older-adolescents).

Patients and methods

Patients

A total of 1,755 newly diagnosed ALL patients aged 1–18 years were enrolled in the TCCSG ALL trials L95-14 [22] (from 1995 to 1999, $n = 597$), L99-15/1502 [23–25] (from 1999 to 2004, $n = 754/254$), and L04-16 (from 2004 to 2006, $n = 150$). All protocols were approved by the institutional review board or equivalent committee at each participating institution. Thirty patients were excluded from this study due to insufficient data related to age. Of the remaining 1725 patients, 373 were aged 10 years or older. The median follow-up period for the 373 patients was 8.8 years.

Risk classification

The risk classification system used in these studies was based on age, leukocyte count at diagnosis, and immunophenotype [22–24]. Risk classification regarding patients 10 years or older is described below. In study L95-14 [22], all patients 10 years of age or older were assigned to a high-risk (HR) group. The indication for allogeneic hematopoietic stem-cell transplantation (HSCT) was a leukocyte count at diagnosis >150000 cells/μl, Ph1, or presence of the *MLL* translocation. Autologous peripheral blood stem-cell transplantation was permitted if an allogeneic HLA-matched donor was unavailable. All HR patients received 18 Gy of cranial irradiation.

In the L99-15/1502 [23–25] and L04-16 studies, upon diagnosis, patients were tentatively assigned to standard risk (SR), intermediate risk (IR), or HR groups. Patients aged 10 years or older with a leucocyte count of <50000 or ≥50000 cells/μl at diagnosis were assigned to IR or HR groups, respectively. For patients with non-T-cell ALL, initial IR patients with prednisolone poor response (PPR ≥1000 blasts/μl in peripheral blood on day 8) were reclassified into the HR group. For T-cell ALL, patients with a very good prednisolone response (VGPR, no blasts in peripheral blood on day 8) were assigned to the IR group and the other patients were assigned to the HR group. Patients with the cytogenetics of Ph1 or 11q23 were assigned to the HR group (Supplementary Figure 1). The indication for allogeneic HSCT was initial HR and PPR of non-T ALL, PPR of T-ALL, Ph1, *MLL* translocation, and failure to enter remission at the end of induction.

Therapies employed in the L95-14, L99-15/1502, and 04-16 studies

The chemotherapy schedule is shown in Supplementary Figure 2 and Tables 1–4. Previous reports provide the details of the treatment regimens of L95-14 [22] and L99-15 [23–25]. From July 2003, the treatment schedule for the HR group of the L99-15 study was amended to that of the L99-1502 study. Berlin–Frankfurt–Münster (BFM)-type block consolidations were administered after induction chemotherapy corresponding to that of the L99-15 study.

S. Ota
Department of Pediatrics, Teikyo University Chiba Medical Center, Ichihara, Japan

Y. Noguchi
Department of Pediatrics, Japanese Red Cross Narita Hospital, Narita, Japan

A. Kikuchi
Department of Pediatrics, Teikyo University, Tokyo, Japan

A. Ohara
Department of Pediatrics, Toho University, Tokyo, Japan

HR1′, HR2′, and HR3′ consolidations of BFM-ALL95 [26] were repeated twice, followed by reinduction and maintenance therapy. Identical chemotherapy treatment schedules were employed by the L04-16 and L99-1502 studies. Patients with leukocyte counts 100000 cells/μl or more received cranial irradiation for prophylaxis with 18 Gy (L95-14 and L99-15/1502) or 12 Gy (L04-16).

Statistical analysis

Fisher's exact test was used to compare differences in the distribution of clinical features among each age group. The duration of event-free survival (EFS) was defined as the time from the initiation of therapy to either treatment failure (relapse, death, or the diagnosis of secondary cancer) or the final day of observation that confirmed the patient was alive. Overall survival (OS) was defined as the time from the initiation of therapy to death from any cause or the time of the last follow-up. The probabilities of EFS and OS were estimated using Kaplan–Meier analysis, and the statistical significance of differences was evaluated using the log-rank test.

Cumulative incidences of relapse were estimated taking into account the competing events of death without relapse and development of a secondary malignancy. To determine the cumulative incidence of non-relapse mortality (NRM), relapse and development of secondary malignancy were considered as competing risk factors. Gray's test was used to assess the statistical significance of age on the cumulative incidences.

Multivariate analysis was performed using the Cox proportional hazard regression model, and the variables considered were patient age groups (younger-adolescents 10–14 years, or older-adolescents 15–18 years), treatment protocols, immunophenotype (T or non-T), initial leukocyte count, and peripheral blast count on day 8. All statistical analyses were performed using the R software 2.13.0 (The R Foundation for Statistical Computing, Vienna, Austria). A 2-sided p value <0.05 was considered statistically significant.

Results

Clinical features of adolescent ALL

Patient characteristics are summarized in Table 1. Compared with patients aged <10 years, older children showed male predominance, high leukocyte count at diagnosis, and increased T-cell phenotype. The frequency

Table 1 Clinical characteristics according to age groups

Characteristics	<10 years	10–14 years	15–18 years	p value
Total (*n*)	1352	332	41	
Study (*n*)				0.66
L95-14	461	122	14	
L99-15/1502	777	187	22	
L04-16	114	23	5	
Gender *n* (%)				0.01
Male	736 (54.6)	206 (62.4)	28 (68.3)	
Female	612 (45.4)	124 (37.6)	13 (31.7)	
WBC at diagnosis *n* (%)				0.01
<50000 cells/μl	885 (65.7)	202 (60.8)	22 (53.7)	
50000–100000 cells/μl	321 (23.8)	76 (22.9)	10 (24.4)	
≥100000 cells/μl	141 (10.5)	54 (16.3)	9 (22.0)	
Immunophenotype *n* (%)				<0.001
Non-T	1235 (92.1)	260 (78.8)	32 (78.0)	
T	106 (7.9)	70 (21.2)	9 (22.0)	
CNS status[a] *n* (%)				0.04
CNS-1	1318 (97.9)	324 (97.6)	37 (90.2)	
CNS-2	15 (1.1)	5 (1.5)	3 (7.3)	
CNS-3	13 (1.0)	3 (0.9)	1 (2.4)	
Cytogenetics[b] *n* (%)	1214	310	37	
High hyperdiploid[c]	255 (21.0)	25 (8.1)	2 (5.4)	<0.001
BCR-ABL1	28 (2.3)	14 (4.5)	1 (2.7)	0.02
TCF3-PBX1	46 (3.8)	25 (8.1)	3 (8.1)	<0.001

WBC white blood cell, *CNS* central nervous system, *PGR* prednisolone good responder, *PPR* prednisolone poor responder

[a] CNS status was evaluated at day 8 [23]

[b] Cytogenetic data were not available for 138 patients <10 years of age, 22 patients 10–14 years of age, and 4 patients of 15–18 years of age

[c] High hyperdiploid was cytogenetically defined as 51 or more modal chromosome number

Table 2 Treatment outcome

Characteristics	<10 years	10–14 years	15–18 years	p*
Patients (n)	1352	332	41	
PB blast on day 8 n (%)				0.88
No blasts	597 (44.2)	137 (41.3)	16 (39.0)	
1–1000 blasts/μl	619 (45.8)	146 (44.0)	18 (43.9)	
>1000 blasts/μl	129 (9.5)	49 (14.8)	7 (17.1)	
Missing data	7 (0.5)	0 (0.0)	0 (0.0)	
CR at end of induction n (%)	1275 (94.3)	308 (92.7)	38 (92.7)	1.0
HSCT in the first CR n (%)	120 (8.9)	60 (18.1)	13 (31.7)	0.06
Allogeneic HSCT (n)	97	48	11	
Autologous PBSCT (n)	19	12	2	
Missing data	4	0	0	
Relapse n (%)	264 (19.5)	93 (29.8)	9 (24.3)	0.59
Median period from diagnosis to relapse, days	688	409	348	0.83
Site of relapse n (%)				0.37
Isolated BM	180 (68.2)	67 (79.8)	8 (88.9)	
Combined BM	26 (9.8)	5 (6.0)	1 (11.1)	
Isolated extramedullary	47 (17.8)	12 (14.3)	0 (0.0)	
Missing data	11 (4.2)	0 (0.0)	0 (0.0)	
Death n (%)	181 (13.4)	87 (26.2)	11 (26.8)	0.86
Remission status at death n (%)				0.40
Death after relapse	135 (74.6)	72 (82.8)	8 (72.7)	
Death in the first CR	46 (25.4)	15 (17.2)	3 (27.3)	
Second malignancy n (%)	18 (1.3)	4 (1.2)	1 (2.4)	0.44

PB peripheral blood, *CR* complete remission, *HSCT* hematopoietic stem-cell transplantation, *BM* bone marrow

* p value for 10–14 and 15–18 years

of high hyperdiploidy was lower in patients aged 10 years or older, whereas the presence of the *TCF3–PBX1* translocation was more frequent. However, most of the characteristics of patients aged 10 years or older were not statistically different between the younger-adolescents (10–14 years) and the older-adolescents (15–18 years). Median of initial leukocyte count was 11000 (500–874000) in the younger-adolescents and 15300 (600–416500) in the older-adolescents. Immunophenotype distribution was similar between the two groups, and 21.2 % of younger-adolescents and 22.0 % of older-adolescents were T-cell ALL, respectively. Incidence of central nervous system (CNS) invasion at diagnosis (CNS-2 and 3) in the older-adolescents was nearly 10 % and higher than that in the younger-adolescents (2.4 %), with statistical significance ($p = 0.03$).

Outcomes of adolescent ALL

The treatment outcomes are shown in Table 2. Early response to treatment, the number of day 8 blasts in peripheral blood, and induction rate were similar between the younger-adolescents and the older-adolescents. HSCT at the first CR (CR1) was performed for 60 (18.1 %) of 332 (including 48 allogeneic HSCTs) younger-adolescents and for 13 (31.7 %) of 41 (including 11 allogeneic HSCT) older-adolescents ($p = 0.06$), while only 120 (8.9 %) of 1352 patients younger than 10 years underwent HSCT at CR1.

The probability of EFS of the 373 patients aged 10–18 years was 66.5 ± 2.5 %. Although the EFS of adolescents was worse than that of <10 years patients (76.5 ± 1.2 %), the EFS was similar in younger-adolescents (66.4 ± 2.6 %) and older-adolescents (67.5 ± 7.4 %) ($p = 0.96$) (Fig. 1a). There was no statistical difference between the probabilities of OS at 8 years, which was 74.2 ± 2.4 % for younger-adolescents and 70.7 ± 7.1 % for older-adolescents ($p = 0.46$) (Fig. 1b).

No significant difference in EFS was observed between the two age groups: L95-14 cohort (68.1 ± 4.3 % for younger-adolescents and 76.9 ± 11.7 % for older-adolescents, $p = 0.51$), L99-15 cohort (68.7 ± 3.8 % for younger-adolescents and 63.2 ± 11.1 % for older-adolescents, $p = 0.47$), and L99-1502 and L04-16 (57.7 ± 6.6 % for younger-adolescents and 62.5 ± 17.1 % for older-adolescents, $p = 0.73$).

The cumulative incidence of relapse at 8 years was 29.2 ± 2.5 % for patients aged 10–14 years and 25.0 ± 7.0 % for those aged 15–18 years ($p = 0.45$) (Fig. 2a). The distribution of relapse sites was not

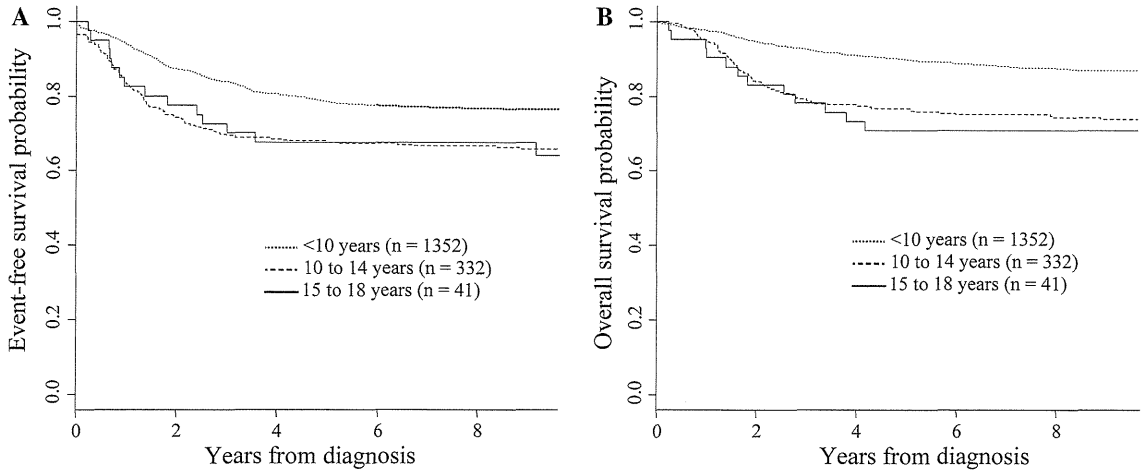

Fig. 1 Analysis of survival probability of patients aged 10 years or older. Estimated probability curves of **a** event-free survival and **b** overall survival are shown according to age groups

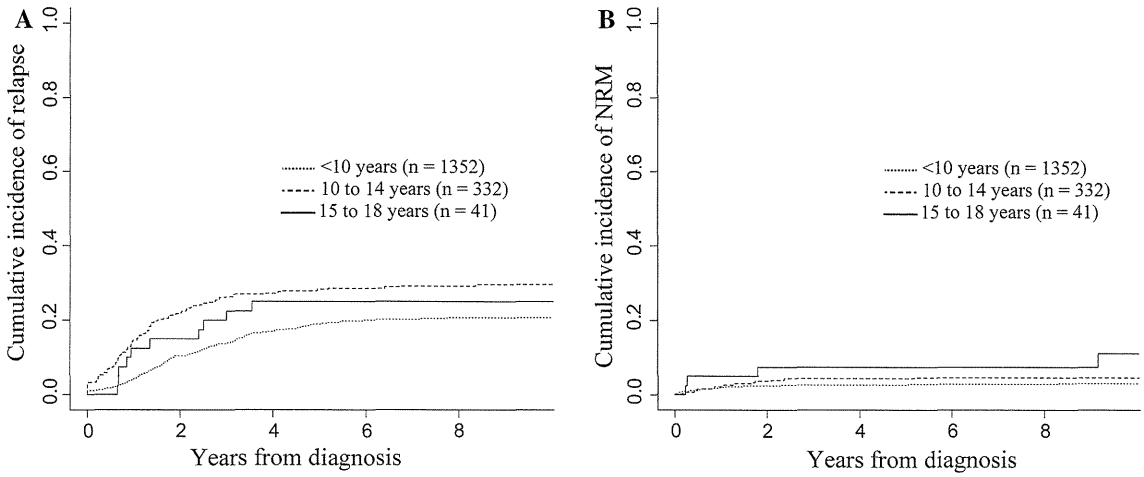

Fig. 2 Relapse and non-relapse mortality incidences of patients aged 10 years or older. Cumulative incidence curves of **a** relapse and **b** non-relapse mortality (NRM) are shown according to age groups

statistically associated with these two age groups, although CNS invasion at diagnosis was more frequently observed in the older age group. There was no isolated extramedullary relapse in older-adolescents, and only one patients with CNS-1 at initial evaluation suffered combined bone marrow and CNS relapse. Thus, the cumulative incidence of CNS-related relapse of older-adolescents was as low as 2.5 ± 2.5 % at 8 years after diagnosis. In the younger-adolescents, 7 (7.5 %) of 93 relapses were CNS-related, which resulted in the cumulative incidence of 2.1 ± 0.8 % at 8 years.

The difference in the cumulative incidence of NRM at 8 years was also not statistically significant (4.6 ± 1.2 % for the younger-adolescents and 7.5 ± 4.2 % for the older-adolescents, $p = 0.15$). Although 11 patients who were aged <10 years died during induction therapy, death during induction therapy was observed in only one of younger-adolescents, and no older-adolescent died during induction therapy. Severe toxicity which resulted in discontinuation of protocol therapy occurred in 4 (1.2 %) of younger-adolescents (including 2 pancreatitis) and 1 (2.4 %) of older-adolescent (due to pancreatitis), whereas 13 (1.2 %) of patients who were aged <10 years could not continue because of toxicity (1 allergy and no pancreatitis).

In the younger-adolescents, 48 patients received allogeneic HSCT during the first CR, and 14 relapses and 5 NRM were observed, which resulted in EFS of 62.4 ± 7.0 %, whereas 3 relapses and no NRM after HSCT were observed in 11 older-adolescents who undertook allogeneic HSCT during the first CR, and EFS at 8 years of these patients was 70.0 ± 14.5 %.

Secondary neoplasms occurred in 4 patients (2 acute myeloblastic leukemia, 1 myelodysplastic syndrome, and

1 tongue carcinoma) among younger-adolescents and 1 patient (breast cancer) among older-adolescents.

Multivariate analysis of EFS did not reveal a statistically significant difference between the younger-adolescents and the older-adolescents (Table 3). Early response to treatment was a significant prognostic factor (hazard ratio for event was 1.81, $p = 0.02$). There was a high probability (86.7 ± 8.8 %) at 8 years of EFS for patients with VGPR in patients aged 15–18 years ($n = 16$).

Table 3 Multivariate analysis of the risk factors for event-free survival in patients aged 10 years or older

Characteristics	Hazard ratio (95 % CI)	*p* value
Patient age		
10–14 years	1	
15–18 years	0.92 (0.53–1.61)	0.77
Treatment		
L95-14	1	
L99-15	0.95 (0.63–1.43)	0.80
L99-1502/L04-16	1.30 (0.79–2.14)	0.30
WBC at diagnosis		
<100000 cells/μl	1	
≥100000 cells/μl	1.25 (0.76–2.04)	0.38
Immunophenotype		
Non-T	1	
T	1.04 (0.96–1.65)	0.85
PB blast on day 8		
<1000 cells/μl	1	
≥1000 cells/μl	1.81 (1.12–2.93)	0.015

WBC white blood cell, *PB* peripheral blood, *CI* cumulative incidence

Discussion

Several studies showed that pediatric-type intensive chemotherapy improves the prognosis of adolescents with ALL, but the outcome of adolescent aged 15 years or older is still not satisfactory [8]. However, there is no consensus on an optimum treatment strategy for these patients because of insufficient data. Therefore, accumulating clinical features is important to resolve this issue. The retrospective analysis of three consecutive TCCSG trials presented in this study demonstrates that long-term outcomes for children aged 15–18 years were comparable with those aged 10–14 years.

Older children with ALL generally exhibit high-risk factors such as high leukocyte count and T-cell phenotype. In this study, we show that patients aged 10 years or older had a higher frequency of the *TCF3-PBX1* fusion in our cohort and that the frequency was not significantly different between younger-adolescents and older-adolescents.

Consistent with the outcomes of adolescent patients with ALL treated according to Dana-Farber Cancer Institute (DFCI) ALL Consortium Protocols [10], the EFS probability curves in TCCSG trials were superimposable for patients aged 10–14 and 15–18 years in our cohort and were reproducible for each treatment protocol. One of the distinctive features of DFCI treatment regimens is the use of intensive asparaginase (total doses of 525000–750000 U/m^2) and anthracycline (60–360 mg/m^2). Although asparaginase is one of the most important agents for the treatment of ALL, adolescent patients have increased rates of asparaginase-related toxicity such as pancreatitis and thrombosis [18, 19, 27]. In contrast, a significant feature of our treatment regimen was intensified

Table 4 Cumulative doses of chemotherapy during induction and consolidation therapy

	CALGB 8811	LALA 94	CCG 1882	FRALLE 93	DFCI 9101/0501	TCCSG L95-14/L99-15/1502
PSL (mg/m^2)	1260	840	1680	2540	1240–7240	2100–3480
DEX (mg/m^2)	140	320	210	140	0–900	84–740
VCR (mg/m^2)	22 (mg)	11.2 (mg)	19.5–37.5	10.5[b]	26	10.5–22.5
L-ASP (U/m^2)	84000	90000	90000–348000	132000	525000–750000	84000–244000
Anthracyclines[a] (mg/m^2)	202	396	86–158	249	60–360	155–243
CPA (mg/m^2)	4200	12500	3000–4000	0	0	2400–4600
Age	16–20 years ($n = 124$)	15–20 years ($n = 100$)	16–20 years ($n = 197$)	15–20 years ($n = 77$)	15–18 years ($n = 51$)	15–18 years ($n = 41$)
EFS	34 % at 7 years	41 % at 5 years	63 % at 7 years	67 % at 5 years	78 % at 5 years	67.5 % at 8 years
OS	46 % at 7 years	45 % at 5 years	68 % at 7 years	78 % at 5 years	81 % at 5 years	70.7 % at 8 years

Chemotherapy during maintenance is not included

[a] Anthracycline was calculated as adriamycin equivalent

[b] Eighteen and 12 mg/m^2 of vindesine (VDS) were scheduled in the FRALLE93 and the TCCSGL04-16, respectively

induction, including cyclophosphamide and block consolidation, with a relatively decreased total dose of asparaginase (84000–244000 U/m^2) and anthracycline (155–243 mg/m^2 of adriamycin equivalent) compared with the DFCI treatment regimen. Summary of total dose of chemotherapeutic agent and outcome of adolescent ALL is listed in Table 4 [10, 15, 16]. Our results demonstrate that TCCSG treatment regimens, which contained moderate doses of asparaginase and anthracycline, achieved comparable outcome for adolescents aged 15–18 years.

Of note, approximately 30 % of our older patients received HSCT during their first remission. Although a previous report suggests an advantage of allogeneic HSCT during the first remission in young adults [28, 29], pediatric-type chemotherapy can minimize the indication for allogeneic HSCT in adolescents [19, 30] to avoid acute and late complications. Our analysis showed that early response to treatment was a strong prognostic predictor in adolescents and the outcomes were excellent for patients with very good responses. Therefore, determining minimal residual disease kinetics [31] may be useful for developing a more refined stratification strategy, including limited indication for allogeneic HSCT.

According to the TCCSG registration data, only 41 (2.4 %) of 1,725 patients were aged 15–18 years. A population-based analysis from the Austrian study group included 6 % of 15 years or older ALL patients among 18 years or younger [11], and children's Oncology Group showed that their clinical trials included 7 % of 15 years or older among younger than 22-year-old ALL patients [8]. In most countries, the percentage of adolescents who enter clinical studies is lower compared with that of younger children [32–35]. Therefore, to clarify comprehensive clinical characteristics of adolescents with ALL, enrollment in clinical studies is essential. Collaboration between pediatric and adult study groups is required to obtain a comprehensive understanding of the characteristics of adolescents and young adults with ALL. More attention should be paid to young adults that are older than 18 years. A prospective collaborative trial is in progress in Japan [36].

Adverse events are generally more problematic in older patients, such as osteonecrosis, thrombotic events, and infection [10, 19]. It is very important to assess how these adverse events affect the quality of life by conducting prospective studies to avoid poor medical compliance of older children.

In conclusion, we suggest that the clinical characteristics and treatment outcomes of adolescents aged 15–18 years are similar to those of children aged 10–14 years. Therefore, our treatment backbone, intensive induction, and block-type consolidation can be adopted for adolescents, although further prospective studies and biological investigations are required for treatment optimization, including a minimized indication for administering allogeneic HSCT.

Acknowledgments We thank Ms. Kaori Itagaki for preparing and refining the protocol data for ALL in the TCCSG. We also thank the pediatricians and nurses who participated in the treatment and follow-up of the patients in this study. This study was supported in part by the Children's Cancer Association of Japan.

Conflict of interest The authors declare that they have no conflict of interest.

References

1. Pui CH, Campana D, Pei D, Bowman WP, Sandlund JT, Kaste SC, et al. Treating childhood acute lymphoblastic leukemia without cranial irradiation. N Engl J Med. 2009;360:2730–41.
2. Schrappe M, Valsecchi MG, Bartram CR, Schrauder A, Panzer-Grumayer R, Moricke A, et al. Late MRD response determines relapse risk overall and in subsets of childhood T-cell ALL: results of the AIEOP–BFM-ALL 2000 study. Blood. 2011;118:2077–84.
3. Conter V, Bartram CR, Valsecchi MG, Schrauder A, Panzer-Grumayer R, Moricke A, et al. Molecular response to treatment redefines all prognostic factors in children and adolescents with B-cell precursor acute lymphoblastic leukemia: results in 3184 patients of the AIEOP–BFM ALL 2000 study. Blood. 2010;115:3206–14.
4. Vrooman LM, Stevenson KE, Supko JG, O'Brien J, Dahlberg SE, Asselin BL, et al. Postinduction dexamethasone and individualized dosing of *Escherichia coli* L-asparaginase each improve outcome of children and adolescents with newly diagnosed acute lymphoblastic leukemia: results from a randomized study—Dana-Farber Cancer Institute ALL Consortium Protocol 00-01. J Clin Oncol. 2013;31:1202–10.
5. Tsuchida M, Ohara A, Manabe A, Kumagai M, Shimada H, Kikuchi A, et al. Long-term results of Tokyo Children's Cancer Study Group trials for childhood acute lymphoblastic leukemia, 1984–1999. Leukemia. 2010;24:383–96.
6. Inaba H, Greaves M, Mullighan CG. Acute lymphoblastic leukaemia. Lancet. 2013;381:1943–55.
7. Horibe K, Saito AM, Takimoto T, Tsuchida M, Manabe A, Shima M, et al. Incidence and survival rates of hematological malignancies in Japanese children and adolescents (2006–2010): based on registry data from the Japanese Society of Pediatric Hematology. Int J Hematol. 2013;98:74–88.
8. Hunger SP, Lu X, Devidas M, Camitta BM, Gaynon PS, Winick NJ, et al. Improved survival for children and adolescents with acute lymphoblastic leukemia between 1990 and 2005: a report from the children's oncology group. J Clin Oncol. 2012;30:1663–9.
9. Harrison CJ. Cytogenetics of paediatric and adolescent acute lymphoblastic leukaemia. Br J Haematol. 2009;144:147–56.
10. Barry E, DeAngelo DJ, Neuberg D, Stevenson K, Loh ML, Asselin BL, et al. Favorable outcome for adolescents with acute lymphoblastic leukemia treated on Dana-Farber Cancer Institute Acute Lymphoblastic Leukemia Consortium Protocols. J Clin Oncol. 2007;25:813–9.
11. Pichler H, Reismuller B, Steiner M, Dworzak MN, Potschger U, Urban C, et al. The inferior prognosis of adolescents with acute lymphoblastic leukaemia (ALL) is caused by a higher rate of treatment-related mortality and not an increased relapse rate: a population-based analysis of 25 years of the Austrian ALL-BFM (Berlin–Frankfurt–Munster) Study Group. Br J Haematol. 2013;161:556–65.
12. Pullen J, Shuster JJ, Link M, Borowitz M, Amylon M, Carroll AJ, et al. Significance of commonly used prognostic factors differs for children with T cell acute lymphocytic leukemia (ALL), as

compared to those with B-precursor ALL. A Pediatric Oncology Group (POG) study. Leukemia. 1999;13:1696–707.
13. Moorman AV, Ensor HM, Richards SM, Chilton L, Schwab C, Kinsey SE, et al. Prognostic effect of chromosomal abnormalities in childhood B-cell precursor acute lymphoblastic leukaemia: results from the UK Medical Research Council ALL97/99 randomised trial. Lancet Oncol. 2010;11:429–38.
14. Secker-Walker LM, Craig JM, Hawkins JM, Hoffbrand AV. Philadelphia positive acute lymphoblastic leukemia in adults: age distribution. BCR Breakpoint Prognostic Significance. Leukemia. 1991;5:196–9.
15. Stock W, La M, Sanford B, Bloomfield CD, Vardiman JW, Gaynon P, et al. What determines the outcomes for adolescents and young adults with acute lymphoblastic leukemia treated on cooperative group protocols? A comparison of Children's Cancer Group and Cancer and Leukemia Group B studies. Blood. 2008;112:1646–54.
16. Boissel N, Auclerc MF, Lheritier V, Perel Y, Thomas X, Leblanc T, et al. Should adolescents with acute lymphoblastic leukemia be treated as old children or young adults? Comparison of the French FRALLE-93 and LALA-94 trials. J Clin Oncol. 2003;21:774–80.
17. de Bont JM, Holt B, Dekker AW, van der Does van den Berg A, Sonneveld P, Pieters R. Significant difference in outcome for adolescents with acute lymphoblastic leukemia treated on pediatric vs adult protocols in The Netherlands. Leukemia. 2004;18:2032–5.
18. Nachman JB, La MK, Hunger SP, Heerema NA, Gaynon PS, Hastings C, et al. Young adults with acute lymphoblastic leukemia have an excellent outcome with chemotherapy alone and benefit from intensive postinduction treatment: a report from the children's oncology group. J Clin Oncol. 2009;27:5189–94.
19. Pui CH, Pei D, Campana D, Bowman WP, Sandlund JT, Kaste SC, et al. Improved prognosis for older adolescents with acute lymphoblastic leukemia. J Clin Oncol. 2011;29:386–91.
20. Chessells JM, Hall E, Prentice HG, Durrant J, Bailey CC, Richards SM. The impact of age on outcome in lymphoblastic leukaemia; MRC UKALL X and XA compared: a report from the MRC Paediatric and Adult Working Parties. Leukemia. 1998;12:463–73.
21. Nakano TA, Hunger SP. Blood consult: therapeutic strategy and complications in the adolescent and young adult with acute lymphoblastic leukemia. Blood. 2012;119:4372–4.
22. Igarashi S, Manabe A, Ohara A, Kumagai M, Saito T, Okimoto Y, et al. No advantage of dexamethasone over prednisolone for the outcome of standard- and intermediate-risk childhood acute lymphoblastic leukemia in the Tokyo Children's Cancer Study Group L95-14 protocol. J Clin Oncol. 2005;23:6489–98.
23. Manabe A, Ohara A, Hasegawa D, Koh K, Saito T, Kiyokawa N, et al. Significance of the complete clearance of peripheral blasts after 7 days of prednisolone treatment in children with acute lymphoblastic leukemia: the Tokyo Children's Cancer Study Group Study L99-15. Haematologica. 2008;93:1155–60.
24. Hasegawa D, Manabe A, Ohara A, Kikuchi A, Koh K, Kiyokawa N, et al. The utility of performing the initial lumbar puncture on day 8 in remission induction therapy for childhood acute lymphoblastic leukemia: TCCSG L99-15 study. Pediatr Blood Cancer. 2012;58:23–30.
25. Kato M, Koh K, Manabe A, Saito T, Hasegawa D, Isoyama K, et al. No impact of enhanced early intensification with intermediate-risk pediatric acute lymphoblastic leukemia: results of randomized trial TCCSG study L99-15. Br J Haematol. 2014;164:376–83.
26. Moricke A, Reiter A, Zimmermann M, Gadner H, Stanulla M, Dordelmann M, et al. Risk-adjusted therapy of acute lymphoblastic leukemia can decrease treatment burden and improve survival: treatment results of 2169 unselected pediatric and adolescent patients enrolled in the trial ALL-BFM 95. Blood. 2008;111:4477–89.
27. Silverman LB, Gelber RD, Dalton VK, Asselin BL, Barr RD, Clavell LA, et al. Improved outcome for children with acute lymphoblastic leukemia: results of Dana-Farber Consortium Protocol 91-01. Blood. 2001;97:1211–8.
28. Gupta V, Richards S, Rowe J, Acute Leukemia Stem Cell Transplantation Trialists' Collaborative G. Allogeneic, but not autologous, hematopoietic cell transplantation improves survival only among younger adults with acute lymphoblastic leukemia in first remission: an individual patient data meta-analysis. Blood. 2013;121:339–50.
29. Wang L, Wang Y, Tang W, Dou HB, Shan JH, Hu J. The superiority of allogeneic hematopoietic stem cell transplantation from unrelated donor over chemotherapy for adult patients with high-risk acute lymphoblastic leukemia in first remission. Int J Hematol. 2013;98:569–77.
30. Isakoff MS, Freyer DR, Bleyer A. Young adults with acute lymphoblastic leukemia treated with a pediatric-inspired regimen do not need a bone marrow transplant in first remission. Blood. 2013;121:5253–5.
31. van Dongen JJ, Seriu T, Panzer-Grumayer ER, Biondi A, Pongers-Willemse MJ, Corral L, et al. Prognostic value of minimal residual disease in acute lymphoblastic leukaemia in childhood. Lancet. 1998;352:1731–8.
32. Stiller CA, Benjamin S, Cartwright RA, Clough JV, Gorst DW, Kroll ME, et al. Patterns of care and survival for adolescents and young adults with acute leukaemia: a population-based study. Br J Cancer. 1999;79:658–65.
33. Nachman J. Clinical characteristics, biologic features and outcome for young adult patients with acute lymphoblastic leukaemia. Br J Haematol. 2005;130:166–73.
34. Bleyer A, Siegel SE, Coccia PF, Stock W, Seibel NL. Children, adolescents, and young adults with leukemia: the empty half of the glass is growing. J Clin Oncol. 2012;30:4037–8.
35. DeAngelo DJ. The treatment of adolescents and young adults with acute lymphoblastic leukemia. Hematol Am Soc Hematol Educ Program. 2005;2005:123–30.
36. Sakura T, Hayakawa F, Yujiri T, Aoyama Y, Kondo E, Fujimaki K, et al. Outcome of pediatric-type therapy for Philadelphia chromosome-negative acute lymphoblastic leukemia (ALL) in adolescents and young adults (AYA): a study by the Japan adult leukemia study Group (JALSG ALL202-U study). Blood. 2012;120:1464 (ASH Annual Meeting Abstracts).

Prognostic impact of gained chromosomes in high-hyperdiploid childhood acute lymphoblastic leukaemia: a collaborative retrospective study of the Tokyo Children's Cancer Study Group and Japan Association of Childhood Leukaemia Study

Although the prognosis of high-hyperdiploid (HHD) acute lymphoblastic leukaemia (ALL) is excellent, relapse occurs in 10–15% of cases (Look *et al*, 1985). A gained chromosome is commonly found (Heerema *et al*, 2000; Kawamata *et al*, 2008), and previous studies reported a correlation between other chromosome combinations and outcomes. The Pediatric Oncology Group (POG) and Children's Oncology Group (COG) demonstrated that the combined gain of chromosomes 4, 10 and 17 (termed as triple trisomy) was associated with a better prognosis (Sutcliffe *et al*, 2005), and POG data suggested that +4 and +10 (termed as double trisomy) patients had a very low risk of relapse (Harris *et al*, 1992).

In this study, we performed a retrospective analysis with the Tokyo Children's Cancer Study Group (TCCSG) cohort as a test set to investigate the relationship between a combination of specific chromosome gains and disease outcomes, and used patients included in the Japan Association of Childhood Leukaemia Study (JACLS) as a validation set.

Paediatric ALL patients (aged 1–18 years old) enrolled in the TCCSG L95-14 (Igarashi *et al*, 2005) (n = 597, 1995–99), L99-15 (Manabe *et al*, 2008; Hasegawa *et al*, 2012; Kato *et al*, 2014) (n = 770, 1999–2003), and JACLS ALL97 (Suzuki *et al*, 2010) (n = 674, 1997–2002) trials were analysed. Based on cytogenetic data obtained with the G-banding test, HHD was defined as a modal chromosome number of 51 or more (Heerema *et al*, 2000), and 186 and 75 HHD patients were analysed from the TCCSG and JACLS cohorts, respectively.

Associations between the gained chromosome pattern and outcomes were investigated with all two combinations of each chromosome in the TCCSG cohort. Combinations with a small number of patients (<25% of all patients, i.e. 47 patients) were excluded. Fifteen combinations were found to have a significant impact on outcome; the association of these combinations and outcomes in the JACLS cohort was analysed for validation (Table SI and Figure S1).

Event-free survival (EFS) was calculated using Kaplan–Meier estimates, and the log-rank test was used to detect significant differences. Multivariate analysis was performed using the Cox proportional hazard regression model. All statistical analyses were performed with the statistical software R (version 2.13.0; The R Foundation for Statistical Computing, Vienna, Austria). A two-sided P-level of <0·05 was considered significant for all analyses.

The characteristics of the paediatric patients with HHD ALL are shown in Table I. The median follow-up period was 2160 d in the TCCSG cohorts. The 6-year EFS and overall

Table I. Characteristics and outcomes of patients with high-hyperdiploidy acute lymphoblastic leukaemia.

	n	Median age at diagnosis, years (range)	P	Median WBC at diagnosis, $\times 10^9$/l (range)	P	6-year EFS	P*
TCCSG cohort							
All	186	4 (1–14)		5·8 (0·3–16·5)		79·7 ± 3·2%	
+11 or +17							
Yes	135	4 (1–14)	0·85	6·2 (0·3–16·5)	0·29	83·2 ± 3·5%	0·027
No	51	3 (1–12)		4·7 (0·8–46·4)		70·8 ± 6·7%	
JACLS cohort							
All	75	3 (1–15)		5·6 (1·6–970)		86·6 ± 4%	
+11 or +17							
Yes	56	3 (1–15)	0·63	5·3 (1·6–970)	0·52	91·1 ± 3·8%	0·045
No	19	4 (1–9)		6·3 (1·9–60·1)		73·0 ± 10·4%	

TCCSG, Tokyo Children's Cancer Study Group; JACLS, Japan Association of Childhood Leukaemia study; WBC, white blood cell count.
*Log-rank test.

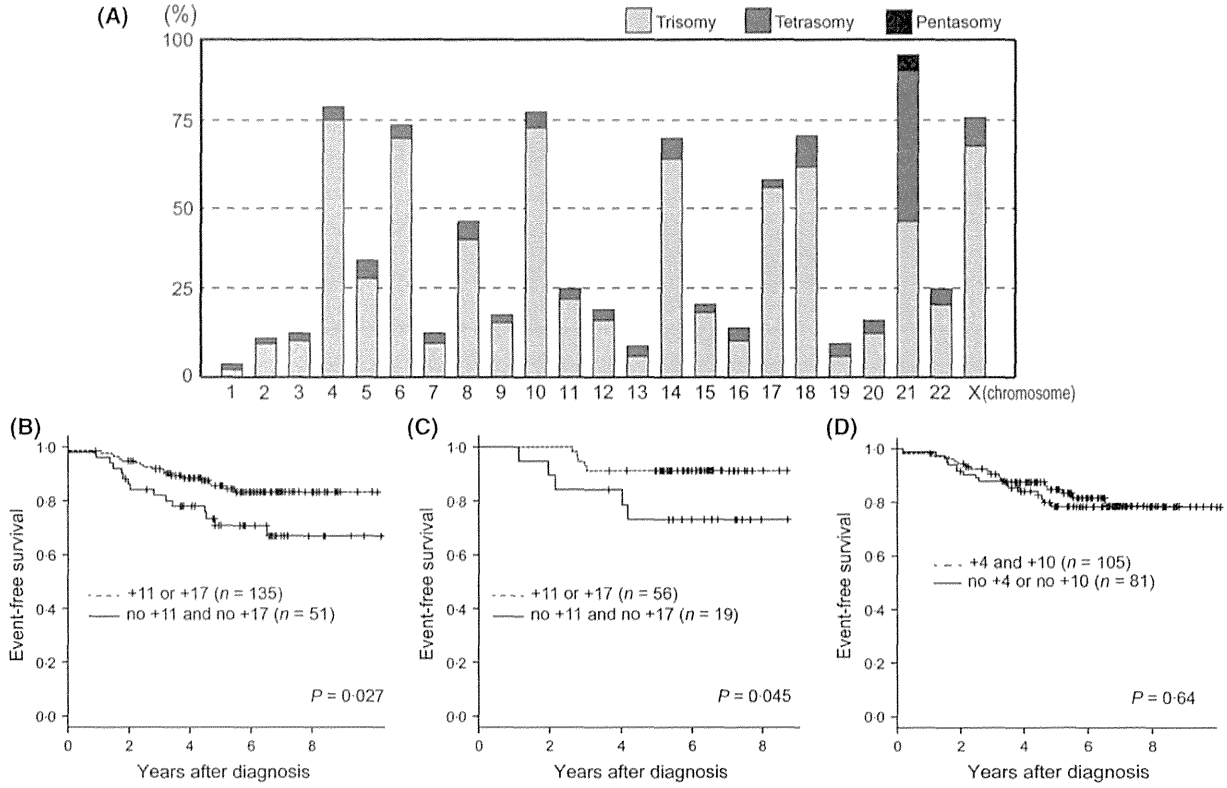

Fig 1. Gained chromosomes in HHD-ALL and their prognostic impact. (A) Frequency of gained chromosomes in 186 HHD-ALL patients in the TCCSG cohort. Event-free survival in the TCCSG and JACLS cohorts is shown. Concurrent absence of a gain of both chromosomes 11 and 17 was associated with poor outcome in the TCCSG cohort (B) and JACLS cohort (C). (D) Event-free survival of ALL patients with or without double trisomy (+4 and +10) in the TCCSG cohort. HHD, high-hyperdiploidy; ALL, acute lymphoblastic leukaemia; TCCSG, Tokyo Children's Cancer Study Group; JACLS, Japan Association of Childhood Leukaemia study.

survival (OS) for HHD patients in the TCCSG cohort was 79·7 ± 3·2% and 91·2 ± 2·3% respectively, compared to 74·4 ± 1·3% and 83·4 ± 1·1%, respectively, for non-HDD patients. The distribution of gained chromosomes in the TCCSG cohort is shown in Fig 1A. In the JACLS cohort, the median follow-up period was 2791 d, and the 6-year EFS and OS was 86·6 ± 4·0% and 97·2 ± 2·0%, respectively.

The absence of +11 and +17 was associated with a poorer outcome in the TCCSG cohort (Table I and Fig 1B). Fifty-one of 186 (27·4%) patients with HHD-ALL and no extra copies of these two chromosomes had a significantly poorer prognosis, with a 6-year EFS of 70·8 ± 6·7% compared to HHD patients with either +11 or +17 (83·2 ± 3·5%, $P = 0·027$). However, no significant difference was observed in OS between the two groups (83·5 ± 5·9% with no +11 and no +17, and 94·3 ± 2·1% with +11 or +17, $P = 0·09$). Mulitvariate analysis failed to identify these chromosome gains as statistically significant due to small sample size (Table SII).

The correlation was concordant with that found in the JACLS cohort. Nineteen of 75 (25·3%) HHD patients had neither +11 nor +17, and EFS was inferior to that of patients with +11 or +17 (73·0 ± 10·4% and 91·1 ± 3·8%, $P = 0·045$) (Fig 1C). No significant difference was observed in age, leucocyte count at diagnosis, or gender between the two groups (Table I).

In contrast to the findings of previous studies by the POG and COG (Harris *et al*, 1992; Sutcliffe *et al*, 2005), double/triple trisomy was not correlated with outcome in our cohort. In the TCCSG cohort, 105 of 186 (56·5%) patients had both +4 and +10, and EFS at 6 years was 81·2 ± 4·2%, whereas EFS of 81 patients without +4 or +10 was 77·8 ± 4·8%, which was not significantly different ($P = 0·64$) (Fig 1D).

Based on the finding that the gain of chromosomes is non-random, it is assumed that the gain of specific chromosomes contributes to leukaemogenesis, while the gain of other chromosomes is a "passenger" event, which is a by-product of leukaemic cell development.

This study showed an association between +11 and +17 and EFS probability in two independent patient cohorts, each of which received different treatments. Data from the POG and COG showed that +4, +10, and +17 was associated with outcome (Heerema *et al*, 2000; Sutcliffe *et al*, 2005), and another report on the Berlin-Frankfürt-Münster study cohort demonstrated that patients with neither +17 nor +18 had

poor outcomes (Kawamata *et al*, 2008). Thus, the gain of chromosome 17 may be the most important 'driver' abnormality in HHD pathogenesis and provide a favourable phenotype. However, it should be noted that no relapse was observed in 21 patients with +11 and +17 of the TCCSG cohort, which suggests that +11 is still associated with better prognosis even in patients with +17.

Some of our findings were inconsistent with those of previous studies. This suggests that the association between the gained chromosome combination and outcome may be influenced by the treatment regimen or ethnicity because most of the enrolled patients in the present study were Asian. The significance of the gain of specific chromosomes in HHD ALL on prognosis should be considered carefully.

Acknowledgement

All authors have no conflict of interest to disclose. We thank Kaori Itagaki for preparing and refining the protocol data for ALL in the TCCSG. We also thank Ms. Noriko Sato for the data management of JACLS ALL97. We thank Dr. Ryo Inuzuka for technical assistance. The TCCSG study was supported in part by the Children's Cancer Association of Japan.

Author contributions

A.M., K.K., H.T., T.T., Y.H., M.T. and A.O. designed the TCCSG study and collected the data. T.I., Y.H., A.S., H.H., M.I., K.H., S.K. and M.O. designed the JACLS study and collected the data. M.K. and T.I. analysed the data. M.K., T.I. and A.M wrote the paper. All authors discussed the results and commented on the manuscript.

Motohiro Kato[1,2]*
Toshihiko Imamura[3]*
Atsushi Manabe[4]
Yoshiko Hashii[5]
Katsuyoshi Koh[6]
Atsushi Sato[7]
Hiroyuki Takahashi[8]
Hiroki Hori[9]
Tomohiko Taki[10]
Masami Inoue[11]
Yasuhide Hayashi[12]
Keizo Horibe[13]
Masahiro Tsuchida[14]
Seiji Kojima[15]
Megumi Oda[16]
Akira Ohara[8]

[1]Department of Cell Therapy and Transplantation Medicine, University of Tokyo, [2]Department of Paediatrics, University of Tokyo, Tokyo, [3]Department of Paediatrics, Kyoto Prefectural University of Medicine, Kyoto, [4]Department of Paediatrics, St. Luke's International Hospital, Tokyo, [5]Department of Developmental Medicine, Osaka University, Osaka, [6]Department of Haematology/Oncology, Saitama Children's Medical Centre, Saitama, [7]Department of Haematology/Oncology, Miyagi Children's Hospital, Sendai, [8]Department of Paediatrics, Toho University, Tokyo, [9]Department of Paediatrics, Mie University, Tsu, [10]Department of Molecular Diagnostics and Therapeutics, Kyoto Prefectural University of Medicine, Kyoto, [11]Department of Haematology/Oncology, Osaka Medical Centre and Research Institute for Maternal of Child Health, Osaka, [12]Department of Haematology/Oncology, Gunma Children's Medical Centre, Maebashi, [13]Clinical Research Centre, National Hospital Organization Nagoya Medical Centre, Nagoya, [14]Department of Haematology/Oncology, Ibaraki Children's Medical Centre, Mito, [15]Department of Paediatrics, Nagoya University, Nagoya, and [16]Department of Paediatrics, Okayama University, Okayama, Japan
E-mail: katom-tky@umin.ac.jp

*These authors contributed equally to this study.

Keywords: high-hyperdiploid, acute lymphoblastic leukaemia, children, prognostic factor, chromosome

First published online 17 March 2014
doi: 10.1111/bjh.12836

Supporting Information

Additional Supporting Information may be found in the online version of this article:

Table SI. Association of gained chromosome combination and outcome.

Table SII. Multivariate analysis of risk factors on the events.

Fig S1. Flow diagram.

References

Harris, M.B., Shuster, J.J., Carroll, A., Look, A.T., Borowitz, M.J., Crist, W.M., Nitschke, R., Pullen, J., Steuber, C.P. & Land, V.J. (1992) Trisomy of leukemic cell chromosomes 4 and 10 identifies children with B-progenitor cell acute lymphoblastic leukemia with a very low risk of treatment failure: a Pediatric Oncology Group study. *Blood*, **79**, 3316–3324.

Hasegawa, D., Manabe, A., Ohara, A., Kikuchi, A., Koh, K., Kiyokawa, N., Fukushima, T., Ishida, Y., Saito, T., Hanada, R. & Tsuchida, M. (2012) The utility of performing the initial lumbar puncture on day 8 in remission induction therapy for childhood acute lymphoblastic leukemia: TCCSG L99-15 study. *Pediatric Blood & Cancer*, **58**, 23–30.

Heerema, N.A., Sather, H.N., Sensel, M.G., Zhang, T., Hutchinson, R.J., Nachman, J.B., Lange, B.J., Steinherz, P.G., Bostrom, B.C., Reaman, G.H., Gaynon, P.S. & Uckun, F.M. (2000) Prognostic impact of trisomies of chromosomes 10, 17, and 5 among children with acute lymphoblastic leukemia and high hyperdiploidy (> 50 chromosomes). *Journal of Clinical Oncology*, **18**, 1876–1887.

Igarashi, S., Manabe, A., Ohara, A., Kumagai, M., Saito, T., Okimoto, Y., Kamijo, T., Isoyama, K., Kajiwara, M., Sotomatsu, M., Sugita, K., Sugita, K., Maeda, M., Yabe, H., Kinoshita, A., Kaneko, T., Hayashi, Y., Ikuta, K., Hanada, R. & Tsuchida, M. (2005) No advantage of dexamethasone over prednisolone for the outcome of standard-

and intermediate-risk childhood acute lymphoblastic leukemia in the Tokyo Children's Cancer Study Group L95-14 protocol. *Journal of Clinical Oncology*, **23**, 6489–6498.

Kato, M., Koh, K., Manabe, A., Saito, T., Hasegawa, D., Isoyama, K., Kinoshita, A., Maeda, M., Okimoto, Y., Kajiwara, M., Kaneko, T., Sugita, K., Kikuchi, A., Tsuchida, M. & Ohara, A. (2014) No impact of enhanced early intensification with intermediate-risk pediatric acute lymphoblastic leukemia: Results of Randomized Trial TCCSG study L99-15. *British Journal of Haematology*, **164**, 376–383.

Kawamata, N., Ogawa, S., Zimmermann, M., Kato, M., Sanada, M., Hemminki, K., Yamatomo, G., Nannya, Y., Koehler, R., Flohr, T., Miller, C.W., Harbott, J., Ludwig, W.D., Stanulla, M., Schrappe, M., Bartram, C.R. & Koeffler, H.P. (2008) Molecular allelokaryotyping of pediatric acute lymphoblastic leukemias by high-resolution single nucleotide polymorphism oligonucleotide genomic microarray. *Blood*, **111**, 776–784.

Look, A.T., Roberson, P.K., Williams, D.L., Rivera, G., Bowman, W.P., Pui, C.H., Ochs, J., Abromowitch, M., Kalwinsky, D. & Dahl, G.V. (1985) Prognostic importance of blast cell DNA content in childhood acute lymphoblastic leukemia. *Blood*, **65**, 1079–1086.

Manabe, A., Ohara, A., Hasegawa, D., Koh, K., Saito, T., Kiyokawa, N., Kikuchi, A., Takahashi, H., Ikuta, K., Hayashi, Y., Hanada, R. & Tsuchida, M. (2008) Significance of the complete clearance of peripheral blasts after 7 days of prednisolone treatment in children with acute lymphoblastic leukemia: the Tokyo Children's Cancer Study Group Study L99-15. *Haematologica*, **93**, 1155–1160.

Sutcliffe, M.J., Shuster, J.J., Sather, H.N., Camitta, B.M., Pullen, J., Schultz, K.R., Borowitz, M.J., Gaynon, P.S., Carroll, A.J. & Heerema, N.A. (2005) High concordance from independent studies by the Children's Cancer Group (CCG) and Pediatric Oncology Group (POG) associating favorable prognosis with combined trisomies 4, 10, and 17 in children with NCI Standard-Risk B-precursor Acute Lymphoblastic Leukemia: a Children's Oncology Group (COG) initiative. *Leukemia*, **19**, 734–740.

Suzuki, N., Yumura-Yagi, K., Yoshida, M., Hara, J., Nishimura, S., Kudoh, T., Tawa, A., Usami, I., Tanizawa, A., Hori, H., Ito, Y., Miyaji, R., Oda, M., Kato, K., Hamamoto, K., Osugi, Y., Hashii, Y., Nakahata, T. & Horibe, K. & Japan Association of Childhood Leukemia Study (2010) Outcome of childhood acute lymphoblastic leukemia with induction failure treated by the Japan Association of Childhood Leukemia study (JACLS) ALL F-protocol. *Pediatric Blood & Cancer*, **54**, 71–78.

Could a citrus keep the haematologist away?

Anaemia has long been recognized as one of the most important prognostic factors in chronic lymphocytic leukaemia (CLL) (Binet *et al*, 1981). Many mechanisms can cause anaemia in CLL including bone marrow infiltration, auto-immunity, cytotoxic therapy, hypersplenism, inflammation, iron deficiency and poor nutritional status (Mauro *et al*, 2002). Among nutritional causes of anaemia, vitamin B9 and vitamin B12 deficiencies are often sought, whereas vitamin C deficiency (hypovitaminosis C) is underestimated (Fain, 2004). Vitamin C, also known as ascorbic acid (AA), is one of the four main antioxidants (AA, vitamin E, selenium and β-carotene) available in human alimentation (Fain, 2004). The pathophysiology of CLL may involve oxidative stress (Sarmento-Ribeiro *et al*, 2012). Because of its role in preventing anaemia and its ability to degrade free radicals and oxidants, we hypothesized that hypovitaminosis C level could be associated with Binet stage C. Herein, we report a single-centre study comparing the blood level of vitamin C in patients with Binet stage A and Binet stage C CLL.

Between June 2012 and November 2012, we performed a prospective exploratory study of the vitamin C plasma level in patients followed for CLL at the Department of Hematology of University Hospital of Tours. In order to compare vitamin C plasma level between low and high burden of disease, we randomly selected 40 patients with Binet stage A CLL and 40 patients with Binet stage C CLL (Binet *et al*, 1981). The only exclusion criterion was ongoing vitamin C supplementation. The following baseline demographical and clinical data were recorded for all of the study patients: age, sex, weight, size, performance status and date of CLL diagnosis. The following blood tests were performed in patients who provided an informed consent: complete blood cell count, reticulocytes, aspartate aminotransferase, serum creatinine level, thyroid-stimulating hormone (TSH), C-reactive protein (CRP), serum iron level, transferrin saturation, ferritin, albumin, folic acid, vitamin B12 and vitamin C serum levels. To protect AA from light and air alteration, blood samples were collected in tubes encased in foil. Results are expressed as mean and confidence intervals. Wilcoxon's test was used to test the comparisons between the two groups. A P value of less than 0·05 was considered significant.

Baseline data and biological test results of the patients are presented in Table I. Stage C patients had lower haemoglobin level than stage A patients (107 g/l, vs. 134 g/l, respectively, $P < 0{\cdot}00005$). Anaemia was mostly normocytic, normochromic and hyporegenerative. Platelet count was also lower in stage C patients than in stage A patients (111×10^9/l, vs. 200×10^9/l, respectively, $P < 0{\cdot}00005$). Thyroid, liver and renal functions, as well as vitamin B9 and serum iron levels, were normal in both groups. CRP and ferritin levels were significantly higher in patients with Stage C (10·0 mg/l, vs. 3·0 mg/l, and 431 μg/l, vs. 117 μg/l, respectively, $P < 0{\cdot}05$ for both comparisons). There was no statistical difference in Vitamin B12 level between the two groups. Vitamin C level was significantly higher in stage A patients than in stage C patients (58·7 μmol/l, vs. 37·7 μmol/l, $P < 0{\cdot}00005$). In total, 22 CLL patients (27·5%) had hypovitaminosis C including three stage A patients (7·5%) and 19 stage C patients (47·5%).

nature COMMUNICATIONS

ARTICLE

Received 29 Jan 2014 | Accepted 21 Jul 2014 | Published 27 Aug 2014

DOI: 10.1038/ncomms5770

Recurrent *CDC25C* mutations drive malignant transformation in FPD/AML

Akihide Yoshimi[1,*], Takashi Toya[1,*], Masahito Kawazu[2], Toshihide Ueno[3], Ayato Tsukamoto[1], Hiromitsu Iizuka[1], Masahiro Nakagawa[1], Yasuhito Nannya[1], Shunya Arai[1], Hironori Harada[4], Kensuke Usuki[5], Yasuhide Hayashi[6], Etsuro Ito[7], Keita Kirito[8], Hideaki Nakajima[9], Motoshi Ichikawa[1], Hiroyuki Mano[3] & Mineo Kurokawa[1]

Familial platelet disorder (FPD) with predisposition to acute myelogenous leukaemia (AML) is characterized by platelet defects with a propensity for the development of haematological malignancies. Its molecular pathogenesis is poorly understood, except for the role of germline *RUNX1* mutations. Here we show that *CDC25C* mutations are frequently found in FPD/AML patients (53%). Mutated CDC25C disrupts the G2/M checkpoint and promotes cell cycle progression even in the presence of DNA damage, suggesting a critical role for CDC25C in malignant transformation in FPD/AML. The predicted hierarchical architecture shows that *CDC25C* mutations define a founding pre-leukaemic clone, followed by stepwise acquisition of subclonal mutations that contribute to leukaemia progression. In three of seven individuals with *CDC25C* mutations, *GATA2* is the target of subsequent mutation. Thus, *CDC25C* is a novel gene target identified in haematological malignancies. *CDC25C* is also useful as a clinical biomarker that predicts progression of FPD/AML in the early stage.

[1] Department of Hematology and Oncology, Graduate School of Medicine, The University of Tokyo, 7-3-1 Hongo, Bunkyo-ku, Tokyo 113-8655, Japan. [2] Department of Medical Genomics, Graduate School of Medicine, The University of Tokyo, 7-3-1 Hongo, Bunkyo-ku, Tokyo 113-8655, Japan. [3] Department of Cellular Signaling, Graduate School of Medicine, The University of Tokyo, 7-3-1 Hongo, Bunkyo-ku, Tokyo 113-8655, Japan. [4] Department of Hematology, Juntendo University School of Medicine, 3-1-3 Hongo, Bunkyo-ku, Tokyo 113-8431, Japan. [5] Department of Hematology, NTT Medical Center Tokyo, 5-9-22 Higashi-Gotanda, Shinagawa-ku, Tokyo 141-8625, Japan. [6] Department of Hematology/Oncology, Gunma Children's Medical Center, 779 Simohakoda, Kitaakebonocho, Shibukawa-shi, Gunma 377-8577, Japan. [7] Department of Pediatrics, Graduate School of Medicine, Hirosaki University, 53 Honmachi, Hirosaki-shi, Aomori 036-8563, Japan. [8] Department of Hematology and Oncology, University of Yamanashi, 1110 Simokawakita, Chuou-shi, Yamanashi 409-3898, Japan. [9] Division of Hematology, Department of Internal Medicine, Keio University School of Medicine, 35 Shinanomachi, Shinjyuku-ku, Tokyo 160-8582, Japan. * These authors contributed equally to this work. Correspondence and requests for materials should be addressed to M.K. (email: kurokawa-tky@umin.ac.jp).

Familial platelet disorder (FPD)/acute myelogenous leukaemia (AML) (MIM601399) is an autosomal dominant disorder with inherited thrombocytopenia, abnormal platelet function and a lifelong risk of the development of a variety of haematological malignancies[1], such as AML, myelodysplastic syndromes (MDS) and myeloproliferative neoplasms. Although inherited *RUNX1* mutations are the cause of the congenital thrombocytopenia, it remains unclear whether a mutation in *RUNX1*, which is generally known to have a dominant-negative effect[2–4], is sufficient to induce the development of haematological malignancies in individuals with FPD/AML. It is also not known whether additional gene mutations are required for the transformation, and, if so, which genes are involved. Given that only 40% of FPD/AML patients develop these neoplasms[5] and that a relatively long period is required for subsequent *RUNX1* mutation-mediated development of neoplasms in FPD/AML, the secondary genetic events may function as a driver to promote malignant transformation. We reasoned that identifying gene mutations responsible for the malignant transformation of FPD/AML would provide indispensable information for addressing these questions. However, only about 30 pedigrees with FPD/AML have been reported so far, and the rarity of this disorder has impeded the establishment of clinical diagnostic criteria and the clinical improvement to refine cancer therapy and to identify biomarkers that would allow detection of patients at risk for the onset of malignancies in FPD/AML.

We collected DNA samples and clinical information of 73 individuals, belonging to 57 pedigrees, who have a history of familial thrombocytopenia and/or haematological malignancies, with the aim of identifying pedigrees with FPD/AML and uncovering recurrent mutations that drive the malignant transformation. Next-generation sequencing and single-cell sequencing strategy suggest that somatic mutation in *CDC25C* may be one of the early genetic events for leukaemic initiation in FPD/AML, and further stepwise acquisition of mutations such as *GATA2* leads to FPD/AML-associated leukaemic progression. These observations shed light on a part of leukemogenesis in FPD/AML.

Results

A novel gene target in haematological disorders. Thirteen patients in 7 pedigrees were diagnosed as having FPD/AML after screening for germline *RUNX1* mutations in 73 index patients; 7 of the 13 patients had developed haematological malignancies, while the other 6 only showed thrombocytopenia (Table 1). Most of the detected *RUNX1* mutations were point mutation in Runt homology domain or frame-shift mutation that lost transactivation domain, consistent with the previous reports[2,4]. As haploinsufficiency of *RUNX1* might cause familial thrombocytopenia with propensity to develop AML[1], we also examined whether the pedigrees have *RUNX1* loss of heterozygosity (LOH) or not. A synchronized quantitative-PCR method[6] and single-nucleotide polymorphism (SNP) sequencing detected no case with LOH in *RUNX1* in our cohort (Supplementary Fig. 1 and detailed in Methods). To systematically identify additional genetic alterations, we utilized whole-exome sequencing for two individuals from the same FPD/AML pedigree who shared a common *RUNX1*_p.Phe303fs mutation and who had developed MDS (subject 20) or myelofibrosis (subject 21) at the age of 37 and 17 years, respectively. In both these patients, the disease had progressed to AML[7]. Validation by Sanger sequencing and/or targeted deep sequencing of candidate mutations in paired tumour/normal DNA samples confirmed 10 (subject 20) and 8 (subject 21) somatically acquired nonsynonymous mutations (Table 2; Supplementary Figs 2–4; Supplementary Methods). Surprisingly, both patients carried the identical somatic *CDC25C* mutation (p.Asp234Gly), which had not been reported previously in human cancers (Fig. 1a,b). Prompted by this finding, we investigated *CDC25C* mutations in other FPD/AML cases by deep sequencing. In total, four of seven affected patients with haematological malignancies had *CDC25C* mutations, of which three carried the same p.Asp234Gly mutation. Moreover, *CDC25C* mutations were detected in an additional three FPD/AML patients who had not yet developed haematological malignancies, although the variant allele fractions (VAFs) were much lower in this group of patients than in those who had already developed haematological malignancies (Fig. 1c; Table 1). Thus, 7 of the 13 FPD/AML patients (53%) harboured a *CDC25C* mutation. *CDC25C* was also screened for mutations in 90 sporadic MDS and 53 AML patients, including 13 MDS and 3 AML cases who carried *RUNX1* mutations. No *CDC25C* mutations were identified in the 90 sporadic cases, except for the p.Ala344Val in an MDS patient bearing a *RUNX1* mutation, indicating that *CDC25C* mutations were significantly associated with germline, but not with somatic *RUNX1* mutations ($P = 0.004$; Supplementary Fig. 5; Supplementary Table 1).

Clonal evolution of FPD/AML. Deep sequencing of individual mutations that had been detected by whole-exome sequencing

Table 1 | Mutational status of *CDC25C* in FPD/AML patients.

Pedigree number	Subject number	RUNX1 mutation	Disease status	Age, years*	CDC25C mutation	VAF (%)
18	20	p.Phe303fs	MDS/AML	37/38	p.Asp234Gly	31.7/45.8
	21		MF/AML	17/18	p.Asp234Gly	31.1/39.0
19	22	p.Arg174*	AML	41	p.His437Asn	39.7
54	65	p.Ser140Asn	MDS	25	—	—
	66		AML	56	p.Asp234Gly	24.2
32	38	p.Leu445Pro	HCL	72	—	—
16	18	p.Thr233fs	Thrombocytopenia	—	p.Asp234Gly	5.9
53	62	p.Gly262fs	MDS	12	—	—
	63		Thrombocytopenia	—	—	—
	67		Thrombocytopenia	—	—	—
57	71	p.Gly172Glu	Pancytopenia†	—	p.Asp234Gly	8.3
	72		Thrombocytopenia	—	—	—
	73		Thrombocytopenia	—	p.Lys233Glu	1.8

AML, acute myeloid leukemia; FPD, familial platelet disorder; HCL, hairy cell leukemia; MDS, myelodysplastic syndrome; MF, myelofibrosis; VAF, variant allele fraction.
*Age at the time of diagnosis of each haematological malignancy is shown.
†Thrombocytopenia, leukopenia and iron-deficiency anemia were diagnosed.

Table 2 | Validated somatic mutations.

Gene symbol	Ref seq_no.	Amino-acid change	Position (hg19)	Base change	Mutation type	SIFT prediction	VAF at MDS/MF (%)	VAF at AML (%)
Subject 20								
AGAP4	NM_133446	p.Arg484Cys	g.chr10:46321905	C->T	Missense	Damaging	13.2	11.5
CDC25C	NM_001790	p.Asp234Gly	g.chr5:137627720	A->G	Missense	Damaging	31.7	45.8
CHEK2	NM_007194	p.Arg406His	g.chr22:29091740	G->A	Missense	Tolerated	14.6	11.1
COL9A1	NM_001851	p.Gly878Val	g.chr6:70926733	G->T	Missense	Damaging	9.6	26.4
DTX2	NM_001102594	p.Pro74Arg	g.chr7:76110047	C->G	Missense	Damaging	18.3	11.2
FAM22G	NM_001170741	p.Ser508Thr	g.chr9:99700727	T->A	Missense	Tolerated	10.2	27.6
GATA2	NM_001145661	p.Leu321His	g.chr3:128202758	T->A	Missense	Damaging	0.0	28.1
LPP	NM_001167671	p.Val538Met	g.chr3:188590453	G->A	Missense	Damaging	9.7	28.8
RP1L1	NM_178857	p.Ser215fs	g.chr8:10480295	insC	Frameshift	Damaging	14.2	12.7
SIGLEC9	NM_014441	p.Ser437Gly	g.chr19:51633253	A->G	Missense	Tolerated	27.4	42.5
Subject 21								
ANXA8L1	NM_001098845	p.Val281Ala	g.chr10:48268018	T->C	Missense	Damaging	30.8	36.8
CDC25C	NM_001790	p.Asp234Gly	g.chr5:137627720	A->G	Missense	Damaging	31.1	39.1
DENND5A	NM_001243254	p.Arg320Ser	g.chr11:9215218	A->C	Missense	Damaging	29.5	37.3
FER	NM_005246	p.Tyr634Cys	g.chr5:108382876	A->G	Missense	Damaging	1.4	30.4
FNDC1	NM_032532	p.Arg189Cys	g.chr6:159636081	C->T	Missense	Damaging	29.3	35.9
OR8U1	NM_001005204	p.Asn175Ile	g.chr11:56143623	A->T	Missense	Damaging	30.0	34.1
PIDD	NM_145886	p.Arg342Cys	g.chr11:802347	C->T	Missense	Damaging	3.3	28.3
ZNF614	NM_025040	p.Glu202Gly	g.chr19:52520246	A->G	Missense	Damaging	28.7	33.7

AML, acute myeloid leukemia; MDS, myelodysplastic syndrome; MF, myelofibrosis; SIFT, sorting intolerant from tolerant; VAF, variant allele fraction.

allowed accurate determination of their VAFs; on this basis, we could establish an inferred model of clonal evolution in terms of individual mutations in subjects 20 and 21 (Fig. 2a,b; Supplementary Fig. 6a,b). Intratumoral heterogeneity was evident at both MDS and AML phases in subject 20. According to the predicted model, a founding clone with a *CDC25C* mutation acquired additional mutations in *COL9A1*, *FAM22G* and *LPP* (group A), followed by the emergence of a *GATA2* mutation (group B), which was associated with leukaemic transformation, whereas the size of another subclone, defined by mutations in *CHEK2* and three other genes (group C), was unchanged. To validate this hierarchical model, single-cell genomic sequencing was performed using genomic DNA of 63 bone marrow cells from subject 20 when the patient was in the AML phase. Assuming that all cells harbour the *RUNX1* mutation, the false-negative rate of the procedure reached 35%, possibly due to biased allele amplification (Online Methods). However, this technique successfully demonstrated that the group A/B and group C mutations were mutually exclusive (Fig. 2c; Supplementary Table 2). To statistically evaluate this possibility, we assumed two hypotheses (H_0: the mutational status of genes in group A/B and group C is independent; H_1: mutations in group A/B and group C are mutually exclusive) and calculated each probability distribution (P_i: probability that the current results as shown in Fig. 2c were obtained under the hypothesis H_i). Our mutational profile data were achieved with a much higher likelihood under H_1 than H_0 (Supplementary Fig. 7 and detailed in Supplementary Methods). Similarly, the clonal architecture for subject 21 was portrayed in Fig. 2b and Supplementary Fig. 6b. In both scenarios, *CDC25C* mutations seemed to represent a founding mutation with the highest VAF, suggesting that the *CDC25C* mutation contributed to the establishment of a founding tumour population as an early genetic event, whereas progression to AML seemed to be accompanied by the appearance of additional mutations, indicating a multistep process in leukemogenesis.

Along with the somatic mutations found in subjects 20 and 21, a *GATA2* mutation was also identified in subject 22 (Fig. 3a). This patient developed AML with multilineage dysplasia, which led to the diagnosis of AML – MRC (myelodysplasia-related changes). Remission-induction therapies were only partially effective and the blast cell count was reduced from 54 to 5.6%, while dysplastic features persisted (Fig. 3b; Supplementary Fig. 8). Allogeneic stem cell transplantation was successfully performed from a human leukocyte antigen-matched unrelated donor and durable complete remission, with 100% donor chimerism, was achieved. During treatment, the VAF of the *GATA2* mutation decreased virtually in parallel with the blast cell percentage, while the VAF of the *CDC25C* mutation hovered at a high level before transplantation. Thus, we hypothesized that the *GATA2* mutation induced leukaemia progression in this patient, whereas the *CDC25C* mutation was associated with the pre-leukaemic status. Another *GATA2* mutation (p.Leu359Val) was found in subject 18, with a VAF (0.94%), who showed only thrombocytopenia without any signs of leukaemia progression and who had a small subclone with a concurrent *CDC25C* mutation (Fig. 3c). Although *GATA2* mutations are detected in a small number of patients with FPD/AML, the findings described above suggest that mutation of *GATA2* is a key factor promoting disease progression in FPD/AML (Fig. 3d).

Biological consequences of *CDC25C* mutations. We next investigated the possible impact of *CDC25C* mutation on clonal selection and evolution. CDC25C is a phosphatase that prevents premature mitosis in response to DNA damage at the G2/M checkpoint, while it is constitutively phosphorylated at Ser216 throughout interphase by c-TAK1 (refs 8–10). When phosphorylated at Ser216, CDC25C binds to 14-3-3 protein[11], leading to sequestration of CDC25C to the cytoplasm and its inactivation. Ba/F3 cells were transduced with retroviruses encoding the wild-type or mutant CDC25C containing each of the individual mutations (p.Asp234Gly, p.Ala344Val, p.His437Asn and p.Ser216Ala), and assayed for the phosphorylation status, 14-3-3 protein-binding capacity and intracellular localization of each of these proteins. The Ser216Ala mutant form

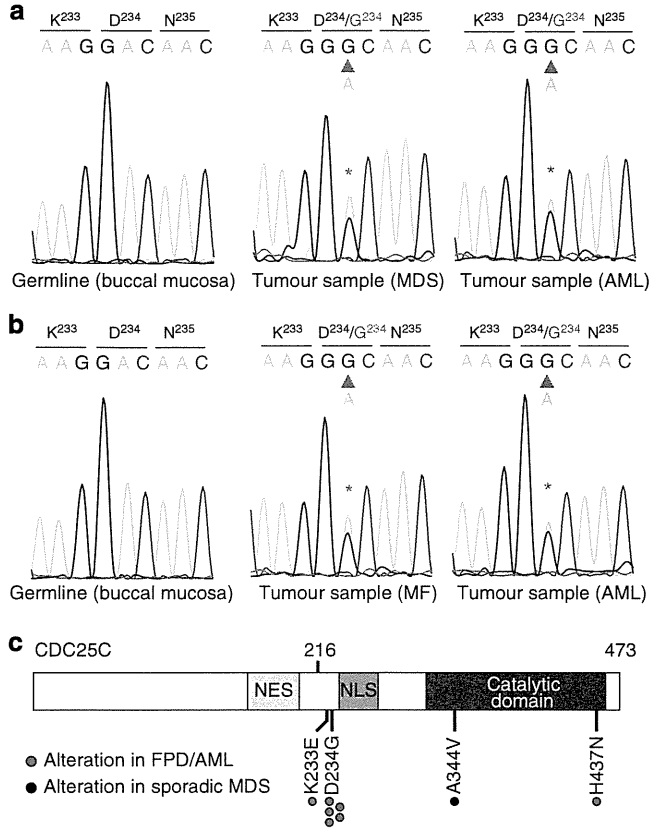

Figure 1 | Mutation in *CDC25C* recurs in cases of FPD/AML. (**a**,**b**) Sanger sequencing of *CDC25C* mutations found in whole-exome sequencing is shown. Both forward and reverse traces were available for each mutation, but only one trace is shown above. The results of buccal mucosa, pre-leukaemic phase and leukaemic phase is demonstrated for subject 20 (**a**) and subject 21 (**b**), respectively. (**c**) The distribution of alterations is shown for the CDC25C protein. NES, a putative nuclear export signal domain between amino acids 177–200; NLS, a putative nuclear localization sequence domain consisting of amino acids 240–244.

of CDC25C, which lacks the phosphorylation site, was used as a negative control. In all of the mutated forms of CDC25C, the capacity for binding to c-TAK1 was reduced (Fig. 4a,b; Supplementary Fig. 9a,b), resulting in decreased phosphorylation of CDC25C at Ser216 (Fig. 4c). Consequently, the mutant proteins failed to bind 14-3-3 protein efficiently (Fig. 4d,e; Supplementary Fig. 8c,d) and remained in the nucleus even during interphase (Fig. 4f; Supplementary Figs 10 and 11). In accordance with these observations, CDC25C mutants enhanced mitotic entry, which was exaggerated by low-dose radiation-induced DNA damage (Fig. 4g,h; Supplementary Fig. 12; Supplementary Methods). These results suggest that mutation of *CDC25C* results in disruption of the DNA checkpoint machinery. Next, we investigated why mutation of *CDC25C* is a frequent genetic event in FPD/AML. It is known that *RUNX1* mutations suppress DNA damage repair and subsequent cell cycle arrest in hematopoietic cells by means of transcriptional suppression of several genes that are involved in DNA repair[12,13]. We confirmed that FPD/AML-associated *RUNX1* mutations have similar effects, as we observed activation of the G2/M checkpoint mechanism in the presence of *RUNX1* mutations (Fig. 4i; Supplementary Fig. 13a,b). We found, however, that introduction of mutations in *CDC25C* resulted in enhanced mitosis entry, despite co-existence of *RUNX1* mutations (Fig. 4i). Therefore, we speculated that compromised DNA damage checkpoint mechanisms caused by mutations in *CDC25C* may contribute to malignant transformation, in concert with increased genomic instability due to *RUNX1* mutations.

Discussion

Whole-exome sequencing, followed by targeted deep sequencing, identified novel aspects of the pathogenesis of malignant transformation in FPD/AML. First, the high frequency of *CDC25C* mutations in FPD/AML underscores their major role in the development of haematological malignancies in FPD/AML patients. To our knowledge, *CDC25C* mutations have not been reported previously and represent a new recurrent mutational target in haematological malignancies, although *CDC25C* mutations have been reported in some solid carcinomas with unknown significance[14,15]. Furthermore, our functional assays support their biological significance, which is characterized by cell cycle progression and premature mitotic entry. Although the 5q31 minimally deleted region, in which CDC25C is located, is frequently detected in MDS, it seems to be associated with other oncogenic mechanisms since our functional assays suggested that *CDC25C* mutations in FPD/AML were gain-of-function type mutations that facilitate the mitotic entry by aberrant accumulation in the nucleus. Impaired DNA repair function mediated by germline *RUNX1* mutation may play a role in the generation of *CDC25C* mutations.

Evaluation of the allelic burden of mutated genes demonstrated that *CDC25* mutations are found with high VAFs in FPD/AML-derived leukaemia and with low VAFs in cases of thrombocytopenia. Our hierarchical model and clonal selection highlighted that mutation of *CDC25C* defines an initial event during malignant transformation and predates subclonal mutations in *GATA2* and other genes. On the basis of the observation that four of the seven FPD/AML patients with *CDC25C* mutations have developed leukaemia and that *CDC25C* mutations were actually detected in the leukaemic subclones, we speculated that a FPD/AML patient with a *CDC25C* mutation, but without clinically evident leukaemia, is at high risk for the onset of leukaemic progression. Examination of the allelic burden of *CDC25C* mutation may thus serve to evaluate the risk of leukaemic progression in patients with FPD/AML.

Among the mutations found in FPD/AML, mutations in *GATA2* were identified in 3 of 13 individuals (subjects 18, 20 and 22). *GATA2* mutations were frequently identified in FPD/AML-derived leukaemia (2/7) and in a patient with thrombocytopenia who had a small subclone bearing a *CDC25C* mutation (1/6). Although reports on the clinical relevance of *GATA2* mutations in myeloid malignancy are limited, several lines of evidence in this respect have recently been reported. *GATA2* mutations are frequently found in a subgroup of patients with cytogenetically normal AML with biallelic *CEBPA* gene mutations[16], which account for ~4% of AML. Germline *GATA2* mutations are also observed in disorders linked to an increased propensity for the development of MDS and AML, including Emberger syndrome, MonoMAC syndrome and dendritic cells, monocytes, B and natural killer cells deficiency[17–20]. The alterations in *GATA2* (leading to p.Leu321His and p.Leu359Val), which were found in FPD/AML patients in this study, are located in the part of the gene encoding the N-terminal and C-terminal zinc-finger domains, respectively (Fig. 3d). Mutations affecting the identical amino acids have been reported in AML patients bearing *CEBPA* mutations and chronic myeloid leukaemia patients in blast crisis[16,21]. Thus, *GATA2* mutation may contribute to AML progression in collaboration with *RUNX1* and/or *CDC25C* mutations. Furthermore, although

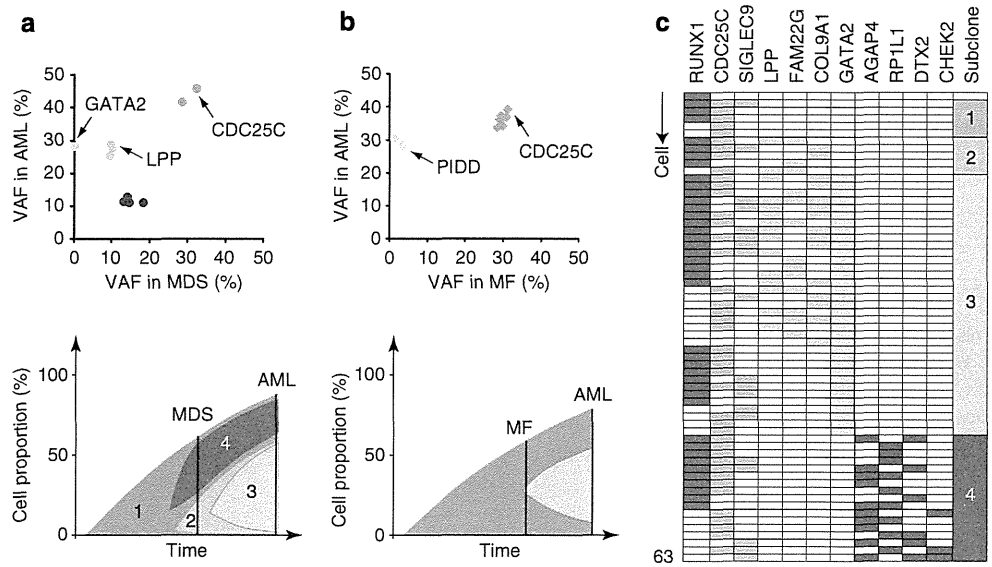

Figure 2 | Clonal evolution of FPD/AML-related myeloid disorders. (**a**,**b**) Observed variant allele fraction (VAF) of validated mutations are listed in Table 2, in both pre-leukaemic and leukaemic phases, are shown in diagonal plots (top) for subject 20 (**a**) and subject 21 (**b**). Predicted chronological behaviours in different leukemia subclones are depicted below each diagonal plot. Distinct mutation clusters are displayed by colour. The vertical axis represents cell proportion of each clone calculated by VAF × 2 (%) (because all the mutations were heterozygous), regarding the whole bone marrow as 100%. (**c**) Mutation status of each bone marrow cell from subject 20 during the acute myeloid leukemia (AML) phase. The vertical axis represents each cell ($n = 63$) and the horizontal axis displays each gene mutation. Coloured columns show that the corresponding cell harbours gene mutation(s) as defined in Online Methods. Subclone numbers shown in the right row correspond to the numbers in the lower figure of **a**.

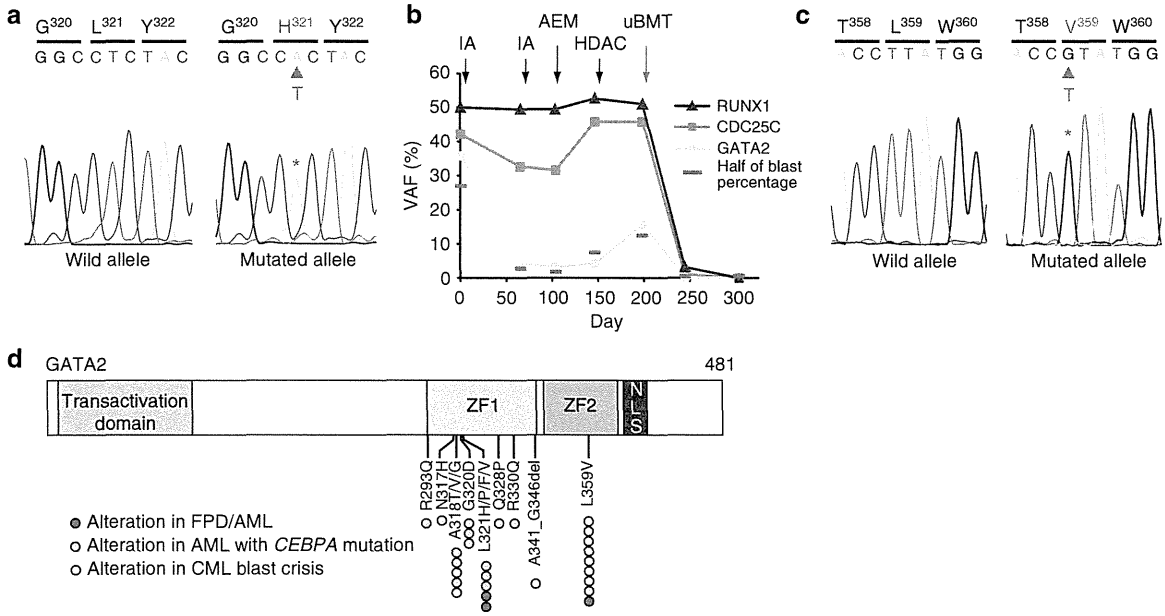

Figure 3 | *GATA2* mutations in FPD/AML. The result of Sanger sequencing for *GATA2* p.Leu321His mutation in subject 22 (**a**) and Leu359Val mutation in subject 18 (**c**) validated with subcloning strategy by methods shown in Supplementary Methods. (**b**) Variant allele fractions (VAFs) of *RUNX1*, *CDC25C* and *GATA2* mutation in subject 22 are demonstrated with the time course of treatment. Half the value of the blast cell percentage, which corresponds to the allele frequency of a heterozygous mutation, is also shown by a red bar. IA, idarubicine + Ara-C; AEM, Ara-C + etoposide + mitoxantrone; HDAC, high-dose Ara-C; uBMT, unrelated bone marrow transplantation. (**d**) Schematic representation of *GATA2* mutations. *GATA2* mutations that were identified in FPD/AML are displayed together with mutations found in AML with *CEBPA* mutation[16] as well as in CML patients in blast crisis[21]. ZF, zinc-finger domain; NLS, a putative nuclear localization sequence domain.

another report identified somatic *CBL* mutation with acquired 11q uniparental disomy as a second hit as being responsible for leukaemic transformation in FPD/AML[22], *CBL* mutations were not detected in our series of FPD/AML samples.

Although the precise pathogenetic roles of *CDC25C* mutations remain unclear, we presume that mutant CDC25C alleles confer a proliferative advantage under certain circumstances in which DNA repair machinery is compromised, such as that mediated by

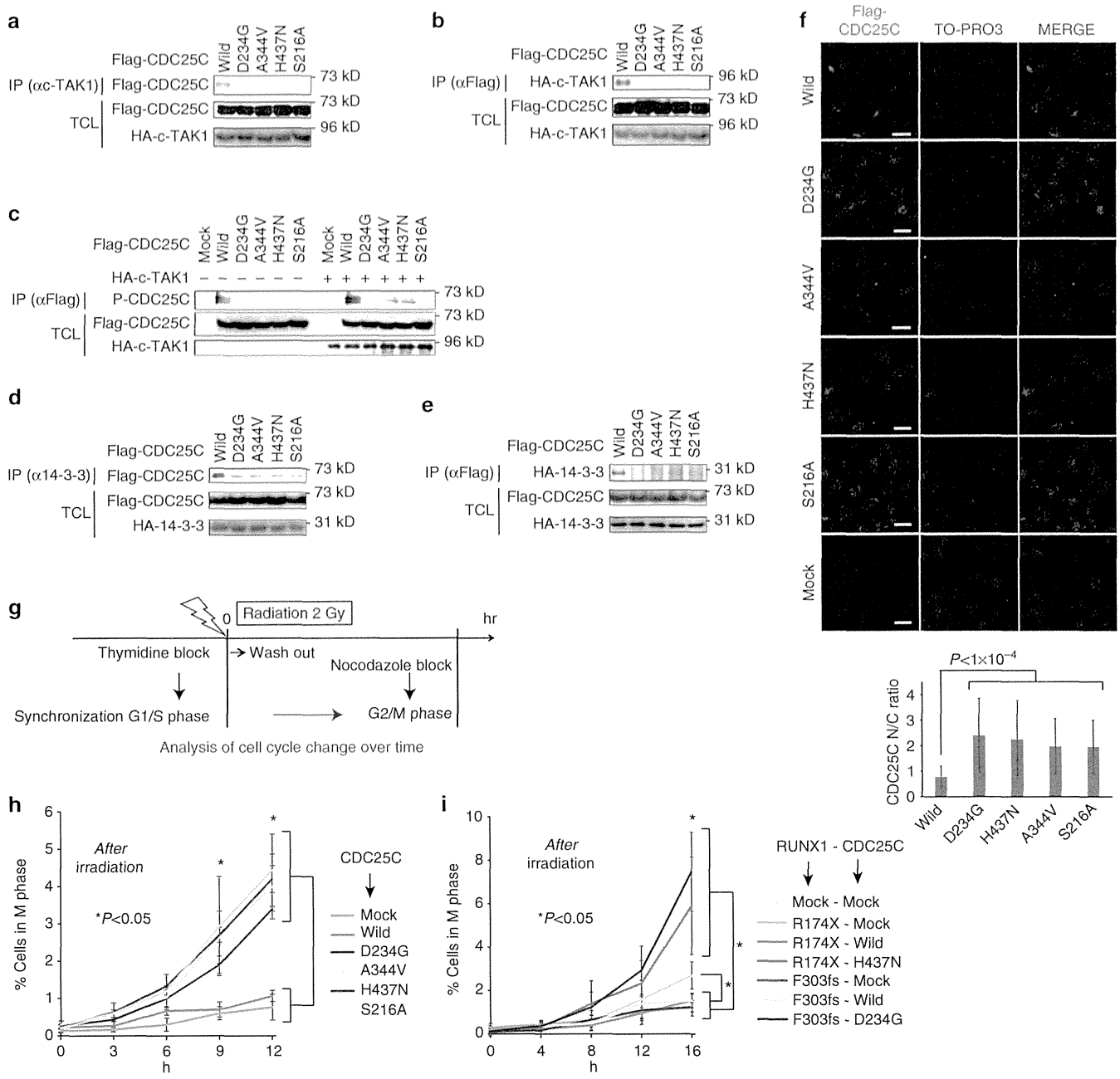

Figure 4 | Mutated CDC25C enhances mitotic entry. (**a**) HEK293T cells were transiently transfected with constructs encoding Flag-tagged CDC25C wild type or mutants, as indicated, and cell lysates were immunoprecipitated with anti-c-TAK1 antibody. Binding capacity of CDC25C was evaluated by western blotting. IP, immunoprecipitation; TCL, total cell lysate. (**b**) Reciprocal immunoprecipitation of **a** using anti-Flag (CDC25C) antibody for immunoprecipitation. (**c**) Left half; cell lysates were immunoprecipitated with anti-Flag antibody. Phosphorylation levels of CDC25C were assessed by phosphorylated-Ser216-specific anti-CDC25C antibody. Right half; the same experiment was performed with cell lysates from HEK293T cells transfected with constructs encoding Flag-tagged CDC25C wild type or mutants and HA-tagged c-TAK1. (**d**) Mutated CDC25C showed reduced capacity for binding to 14-3-3. Cell lysates were immunoprecipitated with anti-14-3-3 antibody and binding capacity of CDC25C was evaluated. (**e**) Reciprocal immunoprecipitation of **d** using anti-Flag (CDC25C) antibody for immunoprecipitation. (**f**) Localization of CDC25C or its mutants was visualized by immunofluorescence. Anti-Flag antibody and Alexa Fluor 555 antibody was used for visualization of CDC25C. N/C ratio of each cell was calculated as detailed in Supplementary Methods and Supplementary Fig. 10. The mean and s.d. of the N/C ratio is presented. Statistical significance of difference was determined by unpaired Student's *t*-test ($n>30$ for each). Scale bar, 10 μm. (**g**) Schematic description of the method used for evaluation of mitotic entry. (**h**) Mitotic entry of CDC25C-mutated cells. Percentage of mutated CDC25C-transduced cells in the M phase was compared with that of wild-type CDC25C-transduced cells. *P* values were calculated using Student's *t*-test and the differences between groups, as indicated, were all statistically significant ($^*P<0.05$) at 10 and 12 h after irradiation ($n=3$). The average and s.d. is presented. (**i**) Mutated RUNX1 and CDC25C were co-expressed in Ba/F3 cells, as indicated, and mitosis entry of these cells was evaluated. The differences between groups, as indicated, were all statistically significant ($^*P<0.05$ at 16 h after washout of thymidine ($n=3$). *P* values were determined using the Student's *t*-test. The average and s.d. is presented.

a germline *RUNX1* mutation. In addition, as Turowski and colleagues reported that CDC25C was involved in S phase entry in addition to mitotic entry[23], release from thymidine-induced G1/S block may be affected by some unknown machinery mediated by mutated CDC25Cs, which might affect the results when we observed G2/M phase fraction of these cells. It is not clear why *CDC25C* mutations are repetitively documented in FPD/AML, but not in sporadic MDS or AML cases. One possibility is that in the presence of a *RUNX1* mutation, as an initial event, an extended period is required before an additional *CDC25C* mutation is acquired. This proposal is supported by the clinical observation that ~40% of patients with FPD/AML develop leukaemia in their 30s[5]; however, the mutational status in *CDC25C* in the reported cohort was unknown.

One of the important problems in the research of FPD/AML is that definitive diagnostic criteria have not been established yet. For this purpose, more extensive studies are required for accumulating clinical characterization, genetic information and functional examination as to whether a *RUNX1* variant in families with thrombocytopenia and/or haematological malignancy is causal[24]. We clarified tentative diagnostic criteria for FPD/AML, which was used in this study (in Methods). Regarding the three missense variants in our study (p.Ser140Asn in pedigree 54, p.Gly172Glu in pedigree 57 and p.Leu445Pro in pedigree 32), Ser140 and Gly172 have been reported to be mutated in sporadic AML and/or MDS cases[25,26]. In addition, induced pluripotent stem cells from a FPD/AML pedigree with p.Gly172Glu recapitulate the phenotype of FPD/AML after hematopoietic differentiation[27]. Ser140 has been also shown to be important for RUNX1 conformation, and a mutation of this site affects hydrogen bonds and results in functional loss[28,29]. Furthermore, all the three missense variants have not been reported in the following SNP database: SNP database (dbSNP) (http://www.ncbi.nlm.nih.gov/projects/SNP), the 1000 Genomes Project (http://www.1000genomes.org), HGVB (http://www.genome.med.kyoto-u.ac.jp/SnpDB/index.html). They were also predicted as 'damaging' by Polyphen-2 (http://genetics.bwh.harvard.edu/pph2/), SIFT (http://sift.jcvi.org/) and PROVEAN (http://provean.jcvi.org/index.php). Therefore, we regarded the pedigrees with these *RUNX1* variants as having FPD/AML in this study. However, regarding pedigree 32 with p.Leu445Pro, we could not completely exclude the possibility of incidental co-occurrence of a possible non-causal *RUNX1* germline variant and hairy cell leukaemia, although co-occurrence of them is supposed to be rare. In addition, we should bear in mind the somatic as well as germline LOH of *RUNX1*, which contributes to thrombocytopenia and/or leukemogenesis in FPD/AML.

In conclusion, our results indicate that FPD/AML-associated leukaemic transformation is due to stepwise acquisition of mutations and clonal selection, which is initiated by a *CDC25C* mutation in the pre-leukaemic phase, and is further driven by mutations in other genes including *GATA2* (Supplementary Fig. 14). The identification of *CDC25C* as the target gene responsible for the leukaemic transformation will facilitate diagnosis and monitoring of individuals with FPD/AML, who are at an increased risk of developing life-threatening haematological malignancy.

Methods

Subjects. Studies involving human subjects were done in accordance with the ethical guidelines for biomedical research involving human subjects, which was developed by the Ministry of Health, Labour and Welfare, Japan; the Ministry of Education, Culture, Sports, Science, and Technology, Japan; and the Ministry of Economy, Trade, and Industry, Japan, and enforced on 29 March 2001. This study was approved by ethical committee of the University of Tokyo and each participating institution. Written informed consent was obtained from all patients whose samples were collected after the guideline was enforced. All animal experiments were approved by the University of Tokyo Ethics Committee for Animal Experiments. The clinical data, peripheral blood sample and buccal mucosa of the patients whose pedigree contained two or more individuals with thrombocytopenia and/or any haematological malignancies were collected from participating institutions. Platelet threshold depended on each institution's judge and any haematological malignancies were allowed. The diagnoses were self-reported. When all the following four criteria were fulfilled, the patient was considered as having FPD/AML in this study: (1) the pedigree has two or more individuals with thrombocytopenia and/or any haematological malignancies; (2) a germline *RUNX1* variant, including missense, nonsense, frameshift, insertion and deletion, is confirmed by Sanger sequencing and a synchronized quantitative-PCR method in at least one family member; (3) the *RUNX1* variant has not been reported in public dbSNP; (4) no germline mutations were detected in the following 16 genes: *GATA2, GATA1, CEBPA, MPL, MYH9, MYL9, GP1BA, GP9, MASTL, HOXA11, CBL, DIDO1, TERT, ANKRD26, GFI1B* and *SRP72*. Regarding the last criterion, 16 genes were selected because they have been reported to be responsible for familial thrombocytopenia and/or haematological malignancies.

Whole-exome sequencing. Genomic DNA was extracted from samples using the QIAamp DNA Mini kit (Qiagen). Exome capture was performed. Enriched exome fragments were subjected to sequencing using HiSeq2000 (Illumina). We removed any potential somatic mutations that were observed in dbSNP (http://www.ncbi.nlm.nih.gov/projects/SNP) or in the 1000 Genomes Project (http://www.1000genomes.org) data. All candidate single-nucleotide variations and indels, which were predicted to be deleterious by the Polyphen-2 algorithm, were validated by deep sequencing and Sanger sequencing. Genomic DNA samples from the buccal mucosa of the two patients (subject 20 and subject 21) were used as references. All candidate somatic mutations were validated by Sanger sequence and deep sequencing using primers listed in Supplementary Tables 3 and 4.

Deep sequencing. Using genomic DNA of the patients as template, each targeted region was PCR amplified with specific primers (Supplementary Table 4). The amplification products from an individual sample were combined and purified with the AMpure XP Kit (Beckman Coulter) and library preparation was carried out using the Ion Xpress Fragment Library Kit (Life Technologies) according to the manufacturer's instructions. The Agilent 2100 Bioanalyzer (Agilent Technologies) and the associated High Sensitivity DNA kit (Agilent Technologies) were used to determine quality and concentration of the libraries. The amount of the library required for template preparation was calculated using the template dilution factor calculation described in the protocol. Emulsion PCR and enrichment steps were carried out using the Ion OneTouch 200 Template Kit v2 DL (Life Technologies). Sequencing was undertaken using Ion Torrent PGM and Ion 318 chips Kit v2 (Life Technologies). The Ion PGM 200 Sequencing Kit (Life Technologies) was used for sequencing reactions, following the recommended protocol. The presence of *CDC25C* and *GATA2* mutations was also validated by a subclone strategy for DNA sequence analysis.

Single-cell sequencing and genome amplification. Single cells were separated from the bone marrow of subject 20 at AML phase using FACSAria II (BD biosciences) (Supplementary Fig. 15a). Each cell was deposited into individual wells of a 96-well plate. Single cells were lysed and whole genome from single cell was amplified using GenomePlex Single Cell Whole-Genome Amplification Kit (Sigma-Aldrich). Mutation status of each gene was analysed by direct sequencing with specific primers (Supplementary Table 5). To improve the sensitivity of this procedure, we used multiple primer sets for detecting a single-nucleotide variation. We estimated the false-negative rate of this procedure based on the ratio of RUNX1 mutation, which is supposed to be observed in all of the cells. The false-negative rate was estimated to be 35% (22 cells out of 63 cells, Supplementary Table 2), which is consistent with the manufacturer's bulletin reporting the allelic dropout of 30%. In light of these results, we regard those cells with at least one gene mutation in a mutational group (coloured in red, orange, green, blue or purple) as being positive for gene mutations of the corresponding group. To assess whether mutations in *LPP, FAM22G, COL9A1* and *GATA2* and mutations in *AGAP4, RP1L1, DTX2* and *CHEK2* were mutually exclusive, we performed a statistical analysis as follows. First of all, we determine a matrix **A** that virtually represents the mutational status of eight genes (1: *LPP*, 2: *FAM22G*, 3: *COL9A1*, 4: *GATA2*, 5: *AGAP4*, 6: *RP1L1*, 7: *DTX2* and 8: *CHEK2*) of 57 cells. Concretely, **A** is defined as follows:

$$\mathbf{A}=\begin{pmatrix} a_{1,1} & \cdots & a_{8,1} \\ \vdots & \ddots & \vdots \\ a_{1,57} & \cdots & a_{8,57} \end{pmatrix} \quad a_{i,j}=\begin{cases} 0: \text{if gene i of cell j is wildtype} \\ 1: \text{if gene i of cell j is mutated} \end{cases} \qquad (1)$$

On the other hand, a matrix **R** indicates data from the actual experimental results of mutational analysis as shown in Fig. 2c. Elements of **R** is provided in

Supplementary Table 2.

$$\mathbf{R}=\begin{pmatrix} r_{1,1} & \cdots & r_{8,1} \\ \vdots & \ddots & \vdots \\ r_{1,57} & \cdots & r_{8,57} \end{pmatrix} \quad r_{i,j}=\begin{cases} 0: \text{if gene i of cell j is wild type} \\ 1: \text{if gene i of cell j is mutated} \\ 2: \text{if mutational status of gene i of cell j is undetermined} \end{cases} \tag{2}$$

Then we assumed two hypotheses: H_0 and H_1.

H_0: the mutational status of genes $1\sim4$ and genes $5\sim8$ is independent. Each matrix elements of **A** are randomly assigned 0 or 1 (at ratio of 1:1) independently of each other.

H_1: mutations in genes $1\sim4$ and genes $5\sim8$ are mutually exclusive, and cells $1\sim40$ harbour mutations of genes $1\sim4$, while cells $41\sim57$ harbour mutations of genes $5\sim8$. In mathematical representation,

$$a_{i,j}=\begin{cases} 0: (5\le i\le 8 \text{ and } 1\le j\le 40) \text{ and } (1\le i\le 4 \text{ and } 41\le j\le 57) \\ 0 \text{ or } 1 \text{ randomely}: (1\le i\le 4 \text{ and } 1\le j\le 40) \text{ and } (5\le i\le 8 \text{ and } 41\le j\le 57) \end{cases} \tag{3}$$

We assumed matrices $\mathbf{A}_0$ and $\mathbf{A}_1$ that represent virtually generated mutational status under the hypotheses H_0 and H_1, and calculate the probability of substantializing **R** for given $\mathbf{A}_0$ and $\mathbf{A}_1$.

$P_0(\mathbf{R}/\mathbf{A}_0)$ and $P_1(\mathbf{R}/\mathbf{A}_1)$ can be calculated for given matrices $\mathbf{A}_0$ and $\mathbf{A}_1$ under the condition as follows:

Probability that we cannot determine whether a cell has mutation in gene X when the cell does not actually have a mutation; 28% (based on our data shown in Supplementary Table 2).

Probability that we judge that a cell has a mutation in gene X when the cell does not actually have a mutation; 5% (because it is very unlikely to happen).

Probability that we can judge correctly that a cell does not have a mutation in gene X when the cell does not actually have a mutation; 67% ($100-28-5=67\%$).

Probability that we cannot determine whether a cell has mutation in gene X when the cell actually has a mutation; 28% (based on our data shown in Supplementary Table 2).

Probability that we judge that a cell has a mutation in gene X when the cell actually has a mutation; 35% (the estimated false-negative rate based on the ratio of *RUNX1* mutation).

Probability that we can judge correctly that a cell has a mutation in gene X when the cell actually has a mutation; 37% ($100-28-35=37\%$).

Put it simply, $\mathbf{P}_0$ represents the probability that one can get the mutational profile R when a cell harbours mutations independently of each other, while $\mathbf{P}_1$ indicates the probability that R is realized under the condition where mutations in gene groups $1\sim4$ and $5\sim8$ are exclusive. Because $\mathbf{A}_0$ and $\mathbf{A}_1$ that meet the hypotheses H_0 and H_1 can be generated innumerably, we conducted a computational simulation to acquire the distribution of P_0 and P_1 by generating $\mathbf{A}_0$ and $\mathbf{A}_1$ 100,000 times. For visibility, horizontal axis is converted to $-\ln(P)$.

Synchronized quantitative-PCR. These experiments were performed mostly as described previously[6]. Briefly, genomic DNA was denatured 95 °C for 5 min and iced immediately. Using the LightCycler 480 Instrument II (Roche), thermal cycling was performed with denatured genomic DNA, forward and reverse primers (Supplementary Table 6), THUNDERBIRD SYBR qPCR mix (TOYOBO). Threshold cycle scores were determined as the average of triplicate samples. We designed 27 primers for *RUNX1* and 3 reproducible primers (that is, primer RUNX-9, RUNX-19 and RUNX-20) were chosen by preparatory experiments. RPL5-2 and PRS7-1 primers, which were authorized previously[6], were also utilized as controls. In addition, genomic DNA extracted from the bone marrow sample of a MDS patient with a chromosome 21 deletion was also examined with the same primers as a control of *RUNX1* locus copy-number loss. Crossing points (Cps) of designed primers were examined by quantitative PCR. *RUNX1* locus copy-number relative to RPL5-2 was calculated using Cps of RUNX-9 and RPL5-2, with RPL5-2 values set at 2. Similar results were obtained when Cps of RUNX-19, RUNX-20 or RPS7-1 values were used.

LOH detection with SNP sequencing. To examine the existence of uniparental disomy, we designed four specific primers to detect nine SNPs in *RUNX1*, which are frequently seen (>40%) (Supplementary Table 7). Direct sequencing was performed with the primers, and heterogeneity of SNPs was examined.

Chemicals and immunological reagents. Thymidine and nocodazole were purchased from Sigma-Aldrich. Anti-CDC25C, anti-phospho-CDC25C (Ser216) and anti-beta-actin antibodies were purchased from Cell Signaling Technology. Anti-HA monoclonal antibody was purchased from MBL. Rabbit anti-Flag monoclonal antibody was purchased from Sigma-Aldrich. Anti-HA was purchased from Roche. Mouse anti-phospho-histone H2AX (Ser139) antibody and Alexa Fluor 488 mouse anti-phospho-H3 (Ser10) antibody were purchased from Merck Millipore. Alexa Fluor 488 rabbit anti-mouse immunoglobulin (Ig)G, Alexa Fluor 488 goat anti-rabbit IgG and Alexa Fluor 555 goat anti-rabbit IgG were purchased from Invitrogen. TO-PRO3 was purchased from Molecular Probes. Rabbit anti-14-3-3 Sigma antibody was purchased from Bethyl laboratories. Sheep anti-c-TAK1 antibody was purchased from Exalpha Biologicals. Anti-sheep IgG-HRP was purchased from RSD. Nonviable cell exclusion was performed by 7-AAD Viability Staining Solution (BioLegend).

Subclone strategy and direct sequencing. Using genomic DNA of the patients as template, each targeted region was amplified by PCR with specific primers (Supplementary Table 4). PCR products were purified with illustra ExoStar (GE Healthcare) and subcloned into *Eco*RV site of pBluescript II KS(−) (Stratagene). Ligated plasmids were transformed into *E. coli* strain XL1-Blue by 45 s heat shock at 42 °C. Positive transformants were incubated on LB plates containing 100 μg ml^{-1} ampicillin supplemented with X-gal (Sigma-Aldrich) and isopropyl β-D-1-thiogalactopyranoside (Sigma-Aldrich). For colony PCR, a portion of a white colony was directly added to a PCR mixture as the DNA template. Insert region was amplified by PCR procedure with T3 and T7 universal primers, purified with illustra ExoStar (GE Healthcare Life Sciences), and sequenced by the Sanger method with T3 and T7 primers using BigDye Terminator v3.1 Cycle Sequencing kit (Applied Biosystems) and ABI Prism 310 Genetic Analyzer (Life Technologies).

Immunoprecipitation and western blotting. These experiments were performed as described previously[30]. Briefly, HEK293T cells were transiently transfected with mammalian expression plasmids encoding Flag-tagged CDC25C and its mutants, HA-tagged 14-3-3 or c-TAK1. All plasmids were sequence verified. After 48 h, cell lysates were collected and incubated with an antibody (anti-HA antibody (1:200, 3 h), anti-Flag antibody (1:200, 3 h), anti-c-TAK1 antibody (1:150, 3 h) and anti 14-3-3 antibody (1:150, 3 h)). After incubation, the cell lysates were incubated with protein G-Sepharose (GE Healthcare) for 1 h. The precipitates were stringently washed with high salt-containing wash buffer and analysed by western blotting. Anti-Flag (HRP-conjugated, Sigma-Aldrich), anti-HA (MBL), anti-HA (HRP-conjugated, Roche), anti-CDC25C (Cell Signaling Technology), anti-phospho-CDC25C (Ser216) (Cell Signaling Technology), anti-c-TAK1 antibody (Exalpha Biologicals) or anti-14-3-3 antibody (Bethyl laboratories) antibodies and Immunostar LD (Wako) was used for detection. Original gel images of western blot analysis are shown in Supplementary Fig. 16.

Cell cycle synchronization and analysis for mitosis entry. After transduction of wild-type CDC25C or its mutated forms to murine lymphoid cell line Ba/F3 cells (RIKEN BioResource Center), double-thymidine block was performed to obtain cell cycle synchronization at G1/S phase. In brief, 2 mM of thymidine was added to the medium. After 16 h, cells were washed and released from the first thymidine for 8 h. A second block was initiated by adding 2 mM of thymidine, and cells were maintained for 16 h. Then thymidine was washed out and the cells were incubated with 1 mM nocodazole with or without 2 Gy of irradiation (Supplementary Fig. 10a). Ba/F3 cells were fixed over time with 75% ethanol in phosphate-buffered saline (PBS) at 4 °C overnight and permeabilized with 2% Triton-X at 4 °C for 15 min. The cells were stained with anti-phospho-H3 (Ser10) Alexa Fluor 488 conjugated antibody (dilution, 1:200) in PBS with 2% fetal calf serum at 4 °C for 30 min and then treated with 5% propidium iodide and 1% RNase in PBS at room temperature (RT) for 30 min. Cell cycle was analysed using a BD LSR II Flow cytometer (BD biosciences) (Supplementary Fig. 15b). To assess the cooperation of *CDC25C* and *RUNX1* mutation, wild-type or mutant (D234G, H437N) pMXs-neo-Flag-CDC25C and mutant (F303fsX566, R174X) pGCDNsam-IRES-KusabiraOrange-Flag-RUNX1 were retrovirally transduced into Ba/F3 cells.

Immunofluorescent microscopic analysis. These experiments were performed as described previously[30]. Briefly, Ba/F3 cells were fixed, permeabilized and blocked. Staining for phosphorylated histone H2AX was performed with anti-phospho-histone H2AX (Ser139) antibody (dilution, 1:500; Merck Millipore) at RT for 3 h. After washing with PBS three times and with 1% bovine serum albumin in PBS, the cells were treated with Alexa Fluor 488 rabbit anti-mouse IgG (dilution, 1:500; Invitrogen) and TO-PRO3 (dilution, 1:1,000; Molecular Probes) for 1 h. The proteins were visualized using FV10i (Olympus) or BZ-9000 (Keyence). The percentage of γH2AX foci-positive cells was determined by examining 100 cells per sample. Three independent experiments were performed. To evaluate the localization of *CDC25C*, Ba/F3 cells were treated with 2 mM thymidine for 12 h and stained. Staining was underwent with anti-Flag antibody or anti-CDC25C antibody at RT for 3 h. After washing, the cells were treated with Alexa Fluor 488 or 555 antibody and TO-PRO3 for 1 h. The mean intensity of CDC25C in the nucleus and cytoplasm of each cell was measured within a region of interest placed within the nucleus and cytoplasm (Supplementary Fig. 10). Similarly, the background intensity was quantified within the region of interest placed outside the cells. All the measurements were performed using the Fluoview FV10i software or ImageJ. The background-subtracted intensity ratio of the nucleus to cytoplasm was calculated in >30 cells in each specimen.

Retrovirus production. The procedures were performed as described previously[30]. Briefly, Plat-E packaging cells were transiently transfected with each retroviral construct using the calcium phosphate precipitation method, and supernatant

containing retrovirus was collected 48 h after transfection and used for infection after it was centrifuged overnight at 10,000 r.p.m.

Statistical analysis. To compare data between groups, unpaired Student's *t*-test was used when equal variance were met by the *F*-test. When unequal variances were detected, the Welch *t*-test was used. Differences were considered statistically significant at a *P* value of <0.05.

References

1. Song, W. J. *et al.* Haploinsufficiency of CBFA2 causes familial thrombocytopenia with propensity to develop acute myelogenous leukaemia. *Nat. Genet.* **23,** 166–175 (1999).
2. Ichikawa, M. *et al.* A role for RUNX1 in hematopoiesis and myeloid leukemia. *Int. J. Hematol.* **97,** 726–734 (2013).
3. Cameron, E. R. & Neil, J. C. The Runx genes: lineage-specific oncogenes and tumor suppressors. *Oncogene* **23,** 4308–4314 (2004).
4. Nickels, E. M., Soodalter, J., Churpek, J. E. & Godley, L. A. Recognizing familial myeloid leukemia in adults. *Ther. Adv. Hematol.* **4,** 254–269 (2013).
5. Liew, E. & Owen, C. Familial myelodysplastic syndromes: a review of the literature. *Haematologica* **96,** 1536–1542 (2011).
6. Kuramitsu, M. *et al.* Extensive gene deletions in Japanese patients with diamond-blackfan anemia. *Blood* **119,** 2376–2384 (2012).
7. Kirito, K. *et al.* A novel RUNX1 mutation in familial platelet disorder with propensity to develop myeloid malignancies. *Haematologica* **93,** 155–156 (2008).
8. Boutros, R., Lobjois, V. & Ducommun, B. CDC25 phosphatases in cancer cells: key players? Good targets? *Nat. Rev. Cancer* **7,** 495–507 (2007).
9. Kastan, M. B. & Bartek, J. Cell-cycle checkpoints and cancer. *Nature* **432,** 316–323 (2004).
10. Peng, C. Y. *et al.* C-TAK1 protein kinase phosphorylates human Cdc25C on serine 216 and promotes 14-3-3 protein binding. *Cell Growth Differ.* **9,** 197–208 (1998).
11. Lopez-girona, A., Furnari, B., Mondesert, O. & Early, P. R. Nuclear localization of Cdc25 is regulated by DNA damage and a 14-3-3 protein. *Nature* **397,** 172–175 (1999).
12. Satoh, Y., Matsumura, I., Tanaka, H. & Harada, H. C-terminal mutation of RUNX1 attenuates the DNA-damage repair response in hematopoietic stem cells. *Leukemia* **26,** 303–311 (2011).
13. Krejci, O. *et al.* p53 signaling in response to increased DNA damage sensitizes AML1-ETO cells to stress-induced death. *Blood* **111,** 2190–2199 (2008).
14. Park, J. *et al.* Mutation profiling of mismatch repair-deficient colorectal cancers using an in silico genome scan to identify coding microsatellites advances in brief mutation profiling of mismatch repair-deficient colorectal cancers using an in silico genome scan to Ide. *Cancer Res.* **62,** 1284–1288 (2002).
15. Vassileva, V., Millar, A., Briollais, L., Chapman, W. & Bapat, B. Genes involved in DNA repair are mutational targets in endometrial cancers with microsatellite instability. *Cancer Res.* **62,** 4095–4099 (2002).
16. Greif, P. A. *et al.* GATA2 zinc finger 1 mutations associated with biallelic CEBPA mutations define a unique genetic entity of acute myeloid leukemia. *Blood* **120,** 395–403 (2012).
17. Ostergaard, P. *et al.* Mutations in GATA2 cause primary lymphedema associated with a predisposition to acute myeloid leukemia (Emberger syndrome). *Nat. Genet.* **43,** 929–931 (2011).
18. Hahn, C. N. *et al.* Heritable GATA2 mutations associated with familial myelodysplastic syndrome and acute myeloid leukemia. *Nat Genet.* **43,** 1012–1017 (2011).
19. Hsu, A. P. *et al.* Mutations in GATA2 are associated with the autosomal dominant and sporadic monocytopenia and mycobacterial infection (MonoMAC) syndrome. *Blood* **118,** 2653–2655 (2011).
20. Dickinson, R. E. *et al.* Exome sequencing identifies GATA-2 mutation as the cause of dendritic cell, monocyte, B and NK lymphoid deficiency. *Blood* **118,** 2656–2658 (2011).
21. Zhang, S.-J. *et al.* Gain-of-function mutation of GATA-2 in acute myeloid transformation of chronic myeloid leukemia. *Proc. Natl Acad. Sci. USA* **105,** 2076–2081 (2008).
22. Hasegawa, D. *et al.* CBL mutation in chronic myelomonocytic leukemia secondary to familial platelet disorder with propensity to develop acute myeloid leukemia (FPD/AML). *Blood* **119,** 2612–2614 (2012).
23. Turowski, P. *et al.* Functional cdc25C dual-specificity phosphatase is required for S-phase entry in human cells. *Mol. Biol. Cell* **14,** 2984–2998 (2003).
24. Michaud, J. *et al.* In vitro analyses of known and novel RUNX1/AML1 mutations in dominant familial platelet disorder with predisposition to acute myelogenous leukemia: Implications for mechanisms of pathogenesis. *Blood* **99,** 1364–1372 (2002).
25. Kohlmann, A. *et al.* Monitoring of residual disease by next-generation deep-sequencing of RUNX1 mutations can identify acute myeloid leukemia patients with resistant disease. *Leukemia* **28,** 129–137 (2014).
26. Chen, C. Y. *et al.* RUNX1 gene mutation in primary myelodysplastic syndrome - The mutation can be detected early at diagnosis or acquired during disease progression and is associated with poor outcome. *Br. J. Haematol.* **139,** 405–414 (2007).
27. Sakurai, M. *et al.* Impaired hematopoietic differentiation of RUNX1-mutated induced pluripotent stem cells derived from FPD/AML patients. *Leukemia.* (epub ahead of print 15 April 2014; doi:10.1038/leu.2014.136).
28. Bravo, J., Li, Z., Speck, N. A. & Warren, A. J. The leukemia-associated AML1 (Runx1)-CBF beta complex functions as a DNA-induced molecular clamp. *Nat. Struct. Biol.* **8,** 371–378 (2001).
29. Akamatsu, Y., Tsukumo, S. I., Kagoshima, H., Tsurushita, N. & Shigesada, K. A simple screening for mutant DNA binding proteins: application to murine transcription factor PEBP2?? subunit, a founding member of the Runt domain protein family. *Gene* **185,** 111–117 (1997).
30. Yoshimi, A. *et al.* Evi1 represses PTEN expression and activates PI3K/AKT/mTOR via interactions with polycomb proteins. *Blood* **117,** 3617–3628 (2011).

Acknowledgements

This work was supported in part by grants-in-aid from the Ministry of Health, Labor and Welfare of Japan (H23-Nanchi-Ippan-104; M. Kurokawa) and KAKENHI (24659457; M. Kurokawa). We thank R. Lewis (University of Nebraska Medical Center) and T. Kitamura (Institute of Medical Science, The University of Tokyo) for providing essential materials; T. Koike (Nagaoka Red Cross Hospital), K. Nara (Ootemachi Hospital), K. Suzuki (Japanese Red Cross Medical Center), H. Harada (Fujigaoka Hospital), Y. Morita (Kinki University), M. Matsuda (PL Hospital), H. Kashiwagi (Osaka University), T. Kiguchi (Chugoku Central Hospital), T. Masunari (Chugoku Central Hospital), K. Yamamoto (Yokohama City Minato Red Cross Hospital), T. Takahashi (Mitsui Memorial Hospital) and T. Takaku (Juntendo University) for providing patient samples; M. Kuramitsu (National Institutte of Infectious Diseases) for providing kind support of synchronized quantitative PCR; and K. Tanaka and Y. Shimamura for their technical assistance.

Author contributions

A.Y., T.T., M.I. and M. Kurokawa analysed genetic materials and performed functional studies. A.T., H.I., M.N., Y.N. and S.A. were involved in sequencing and/or functional studies. M. Kawazu, T.U. and H.M. took part in whole-exome sequencing, deep sequencing and bioinformatics analyses of the data. A.Y., T.T., M.I., H.H., K.U., Y.H., E.I., K.K. and H.N. collected specimens. A.Y. and T.T. generated figures and tables. M. Kurokawa designed and led the entire project. A.Y., T.T. and M. Kurokawa wrote the manuscript. All authors participated in the discussion and interpretation of the data.

Additional information

Accession codes: Sequence data for FPD/AML patients has been deposited in GenBank/EMBL/DDBJ sequence read archive (SRA) under the accession code SRP043031

Supplementary Information accompanies this paper at http://www.nature.com/naturecommunications

Competing financial interests: The authors declare no competing financial interests.

Reprints and permission information is available online at http://npg.nature.com/reprintsandpermissions

How to cite this article: Yoshimi, A. *et al.* Recurrent *CDC25C* mutations drive malignant transformation in FPD/AML. *Nat. Commun.* 5:4770 doi: 10.1038/ncomms5770 (2014).